Stable isotope and gas properties of two ice wedges from Cape Mamontov Klyk, Laptev Sea, Northern Siberia

T. Boereboom[1], D. Samyn[1,*], H. Meyer[2] and J-L. Tison[1]

[1]{Laboratoire de Glaciologie, Université Libre de Bruxelles, Belgium}

[2]{Alfred Wegener Institute for Polar and Marine Research, Research Unit Potsdam, Potsdam, Germany}

[*]{now at: Dpt of Mechanical Engineering, Nagaoka University of Technology, Nagaoka, Japan}

Correspondence to: T. Boereboom (thierry.boereboom@ulb.ac.be)

Abstract

This paper presents and discusses the texture, fabric, water stable isotopes ($\delta^{18}O$, δD) and gas properties (total gas contents ~~of total gas~~, O_2, N_2, Ar, CO_2, and CH_4 mixing ratios) of two climatically contrasted (Holocene vs. Pleistocene) ice wedges (IW-26 and IW-28) from Cape Mamontov Klyk, Laptev Sea, in Northern Siberia. The two ice wedges display contrasting structures: one being of relatively "clean" ice and the other showing clean ice at its centre as well as debris-rich ice on both ~~its~~ sides (referred to as "ice-sand wedge"). ~~A comparison of gas properties, crystal size, fabrics and stable isotope data ($\delta^{18}O$ and δD)~~ Our multiparametric approach allows discriminating between three different ice facies ~~of ice~~ with specific ~~paleoenvironmental~~ signatures, suggesting different climatic and environmental conditions of formation and various intensities and nature ~~rates~~ of biological activity. More specifically, crystallography, total gas content and gas composition reveal variable ~~intensities~~ levels of meltwater infiltration and ~~show the impact of biological processes with~~ contrasting contributions from anaerobic and aerobic conditions to the biological signatures. Stable isotope data are shown to be valid for discussing changes in paleoenvironmental conditions and~~/or decipher~~ in the temporal variation of the different moisture sources for the snow feeding into the ice wedges infillings~~with time~~. Our data set also give further support to the previous assumption that the ice wedge IW-28 was formed in Pleistocene and the ice wedge

IW-26 in Holocene times. This study sheds more light on the conditions of ice wedge growth under changing environmental conditions.

1 Introduction

~~There is growing evidence that the permafrost environment has been changing recently (Brown and Romanovsky, 2008; IPCC, 2007; Wagner and Liebner, 2009). This points to the urgent need to study permafrost and its main physical and biogeochemical properties in order to follow the transformations of this widespread ecosystem and to quantify its contribution to the global greenhouse effect. The periglacial environment has become increasingly wet and the depth of the permafrost table has increased in the last decades (Brown and Romanovsky, 2008; Kolchugina and Vinson, 1993; Nelson and Anisimov, 1993). This increase of water in the liquid state is thought to stimulate methane production which is a greenhouse gas 23 times more effective than carbon dioxide (e.g. Lambert et al., 2006).~~

~~Studies of ice properties within ice wedges are a rich source of information in several aspects: facies, texture and fabric studies provide details on genetic processes (Black, 1954, 1978, 1963; Corte, 1962; Shumskii, 1964; Gell, 1976, 1978a, 1978b; Samyn et al., 2005) while stable water isotopes (δ^{18}O and δD) additionally reveal information about paleotemperatures and paleoenvironmental conditions since ice wedges are built from both the winter snow and the spring meltwater (Meyer et al., 2002a, 2002b; Lauriol et al., 1995; Vasil'chuk and Vasil'chuk, 1998; Vaikmäe, 1989; Dereviagin et al., 2002; Raffi et al., 2004), provided fractionation processes from phase changes are discussed and secondary processes shown to be limited.~~

Ice wedges are a common geomorphological feature of permafrost areas in the Northern Hemisphere and widespread in Alaska, Canada and Siberia. The analysis of ice wedges properties is therefore commonly used to provide proxy-data for paleoclimatic and paleoenvironmental reconstructions. First, the isotopic signature (δ^{18}O or δD) of the ice is thought to reflect the isotopic characteristics of the winter precipitation which are a function of the temperature at the site (Dereviagin et al., 2002; Lauriol et al., 1995; Meyer et al., 2002a, 2002b; Raffi et al., 2004; Vaikmäe, 1989; Vasil'chuk and Vasil'chuk, 1998). As an example, recent ice wedges in Northeast Siberia show δ^{18}O/δD values between -25‰/-190‰ and -20‰/-140‰ (Opel et al., 2011), while younger Holocene ice wedges values range between -26‰/-195‰ and -22‰/-175‰ and older Holocene ice wedges are -26‰/-202‰ to

-24‰/-190‰ (Wetterich et al., 2008). The Pleistocene isotopic signature in the same area clearly differs by decreases of approximately 5‰ and 35‰ in $\delta^{18}O$ and δD, respectively (Popp et al., 2006) showing $\delta^{18}O/\delta D$ values between -33‰/-250‰ and -31‰/-245‰ (Wetterich et al., 2008) with minima from the Last Glacial Maximum (-35‰/-290‰) as documented in a recent overview from Wetterich et al. (2011).

Co-isotopic approaches, use the deuterium excess (*d*) as a tracer for changes in the atmospheric source. For example, Meyer et al. (2010b), who identified the Younger Dryas cold event in Northern Alaskan ice wedges, also brought to the light a rapid reorganization of the Arctic atmospheric circulation following the opening of the Bering Strait, with *d*-transitions from about 6 ‰ to about 9 ‰, as also observed in the North GRIP deep ice core.

Other ice wedge properties can be useful to understand and reconstruct the environmental condition prevailing during ice wedge genesis. St-Jean et al. (2011) recently used ice crystallography, bubble content, gas composition and stable O-H isotopes of ground ice to identify contrasting genetic processes between ice wedges formed during the Late Pleistocene period under cold and dry climatic conditions and ice wedges formed during the Holocene in warmer and wetter conditions. Ice wedges formation primarily results from cyclic frost-cracking and crack infilling by ice (e.g. Mackay, 1974). The cracking results from the thermal contraction of the soil the winter (Lachenbruch, 1962) and the origin of the ice infilling can be attributed to several sources (or mixture of sources) such as: a) unmodified winter snow, b) hoarfrost accretion during winter and c) snow melt infiltration in spring, subsequently refreezing in the crack to form “ice veins” (e.g. Lauriol et al., 1995; Opel et al., 2011; St-Jean et al., 2011). In their work, St-Jean et al. (2011) contrast a Pleistocene ice wedge in which the ice filling rather results from dry snow compaction or hoarfrost accretion and an Holocene ice wedge in which liquid water infiltration and refreezing dominates.

Ice wedges incorporate variable amounts of sediment depending on the sediment, snow and/or water availability at a given time. Frost cracks can be completely filled by blown sediments in very dry conditions forming a “sand wedge” (e.g. Berg and Black, 1966) or can be filled-in by successive ice veins and sediments layers as described in Meyer et al. (2002a) or in Romanovsky (1976). This latter type of structure will be here referred to as an “ice-sand wedge” (also termed “composite wedge”).

In this paper, we propose a multi-parametric~~er~~ approach ~~using~~ including stable isotope composition, total gas content, gas composition, ~~texture and~~ as well as textures and fabrics ~~of~~

to study two specific ice wedges from the Laptev Sea region ~~coast~~. These two ice wedges were sampled from a cliff in the framework of the project "Process studies of permafrost dynamics in the Laptev Sea"~~the research project "Process studies of permafrost dynamics in the Laptev Sea"~~, which aimed~~which~~ to address ~~addressed~~ the paleoenvironmental history of the Cape Mamontov Klyk area (Bobrov et al., 2009; Müller et al., 2009; Schirrmeister et al., 2008). These specific ice wedges were chosen for this study due to their contrasting ages (Holocene vs. Pleistocene) as indicated by their stable isotope signature and stratigraphic position in a dated regional sequence. The aim of the study is two-fold: a) to improve our understanding of the imprint of the contrasted Holocene/Pleistocene climatic and environmental conditions on the ice wedge properties and infilling processes and b) to interpret the specific deuterium excess signature of the two ice wedges in terms of potential changes in atmospheric moisture sources.~~. We use total gas content and gas composition measurements as a tool to describe the various physical and biological processes involved in ice-wedge genesis and the prevailing environmental conditions. We combine those results to a co-isotopic analysis (δD *vs.* $\delta^{18}O$) of the samples to show that δ- and deuterium excess (*d*) values of our ice wedges can be interpreted in terms of contrasting paleoclimatic and paleoenvironmental conditions between the Pleistocene and the Holocene.~~

2 Study area and ice wedge description

The two studied ice wedges are part of a~~n outcrop~~ coastal bluff on the Laptev Sea coast, about 300 km west from the Lena Delta (73°36' N; 117°10' E, Fig. 1). This area belongs to the subarctic tundra in a region of continuous permafrost, with a thickness of 400-600 m (Yershov, 1989). The active layer shows a maximum thaw depth of 0.2-0.5 m in July. The area is dominated by a continental arctic climate with long severe winters and short cold summers.

The cliff from which the ice wedges originate is subdivided into four different sedimentological units (A to D, from old to young; Fig. 2a) and described in detail by Schirrmeister et al. (2008). From the bottom of the cliff to its ~~summit~~top, we distinguish a lower sand unit (unit A) that consists of yellowish-grey, irregularly-laminated fine-grained sand, lacking visible plant remains. Grass roots in the uppermost horizon of this unit were dated to 44.5 ky (Schirrmeister et al., 2008). Above, unit B consists of an alternation of four cryoturbated peat-rich horizons and irregularly-laminated, dark-grey silty to fine-grained

sandy interbeds. Unit C is known as ~~the~~ "Ice Complex", ~~that is~~ a type of ice-rich permafrost deposit of Late Pleistocene age widespread in Arctic Siberia attributed at this site to the Sartan period (Schirrmeister et al., 2008). The Ice Complex deposits are composed of alternating mineral-rich (greyish) and organic-rich (brownish) sediment layers. The upper unit (unit D) consist of peat soils of Holocene age originating from fillings of small thermokarst or polygonal ponds developed on top of the Ice Complex or from Holocene thermoerosional or fluvial deposits.

Ice wedge 26 (IW-26, Fig. 2~~a~~b) was sampled within unit C in the upper part of the cliff, at 18.6 m above sea level, and is therefore embedded within ~~the~~late Pleistocene Ice Complex sediments (Schirrmeister et al., 2008). IW-26 is about ~~only~~ 1.6 m in width and about 2.5 m in height are visible. Sampling was performed across the full ice-wedge width, ~~and~~ approximately 1.2 m below the surface. The ice samples consisted~~s~~ of foliated grey to white, and in parts yellowish, ice with small (millimetric) gas bubbles ~~(millimetric)~~. The wedge ice shows a low content of mineral particles and organic matter (fine-disperse individual particles or thin layers following the foliation).

The second ice wedge studied in this paper, IW-28 (Fig. 2c~~b~~), has been attributed to unit A in the lower part of the cliff and was sampled at 1 m above sea level. It developed in sandy sediments. IW-28 is up to 5 m wide in its upper part at the top of the cliff. The ice wedge is laterally associated with an ice-sand wedge (ISW-28), a portion of which was also sampled (Fig. 2c~~b~~, left of sampling box). In the central section, the wedge ice has a white and milky appearance, and small millimetric gas bubbles are frequent (Fig. 3~~4~~d). The mineral content and the organic matter contents are both low, with particles dispersion similar to that in IW-26 and foliation layers that are 1-3 mm wide. For the ice-sand wedge portion, the ice is mixed with a significant amount of fine-grained sediments alternating with clean ice layers.

3 Sampling and analytical methods

The ice wedges were sampled as ice blocks using a chain saw, in horizontal transects covering the entire ice-wedge width and partly including the ice-sand wedge section from now on referred to as ISW-28 (Fig. 2c). Samples used in this paper for fabric, texture, gas and stable isotope analyses are derived from horizontal sections (±1.5 cm thickness) in the ~~upper~~ top part of the blocks extracted from the ice wedge.

Horizontal thin sections were prepared using a traditional biological microtome (Leitz 1400) for the clean ice and a diamond-wire saw (Well 6234) for the debris-laden ice, following the standard procedures from Langway (1958) and Tison (1994), respectively.

Crystal-size determination was performed using two different techniques. The first was the mean linear intercept method developed by Pickering (1976). The number of grain boundaries $(\bar{N})$ crossed by a random linear traverse of length $(\bar{L})$ across the thin section was averaged over many traverses. The mean grain diameter $(\bar{d})$ was estimated using the following equation: $\bar{d} = \bar{N}/\bar{L}$. The second method, proposed by Jacka (1984), estimates the mean diameter by counting the number of entire crystals in a known area and assuming a circular cross-section following the equation $\bar{d} = \sqrt{4A/\pi N}$, where A is the area of thin section studied and N is the crystal count.

Stable water isotopes were measured at high resolution (approximately every centimeter) with a Finnigan MAT Delta-S mass spectrometer at the Alfred Wegener Institute, Research Unit Potsdam using equilibration techniques. Hydrogen and oxygen isotope ratios are ~~given~~ presented as per mil difference relative to V-SMOW (‰, Vienna Standard Mean Ocean Water), with internal 1σ errors better than 0.8‰ and 0.1‰ for δD and $\delta^{18}O$, respectively (Meyer et al., 2000).

Gas inclusions entrapped in the ice were analysed for their total gas volume (27 samples) and gas composition (CO_2, O_2, N_2, Ar, and CH_4). Gas composition (CH_4 = 24 samples, Ar = 7 samples, other gases = 30 samples) was measured by gas chromatography (Interscience Trace GC) using an FID detector for CO_2 and CH_4 and a TCD detector for O_2, Ar and N_2. Between 20 to 35 grams of sample were used for each measurement. For CO_2, O_2, Ar and N_2, we used the dry-extraction technique described in Raynaud et al. (1982) and Barnola et al. (1983). For CH_4, we used the melting-refreezing procedure described in Raynaud et al. (1988) and Blunier et al. (1993). The levels of precision of the measurements ~~were~~ are 2.5% for CO_2, 0.4% for O_2 and N_2, 2% for Ar and 3% for CH_4. The total gas content (27 samples) was determined using a Toepler pump and a melting-refreezing extraction technique described in Martinerie et al. (1994). The precision of the measurements ~~was~~ is $\leq$ 5%.

The limited amounts of ice provided for the gases and fabrics analyses did not yield enough material to perform a full granulometric analysis of the sediment inclusions, which is nevertheless beyond the scope of this paper. At a later stage of the interpretation, however, ~~The~~ the residual sediments collected after the gas analyses have been treated by HCl (1 mol.l^{-}

[1]) and H_2O_2 (30%) for qualitative detection of calcium carbonate or organic matter, respectively.

4 Results

4.1. Stable ^{18}O and ^{2}H isotopes

Ice wedge IW-26 shows $\delta^{18}O$ values ranging between -22.6‰ and -25.8‰ and δD values between -170‰ and -191‰, respectively (Fig. ~~3a~~4a). The IW-26 samples plot on a slope of 6.63 in the ~~co-isotopic~~D-^{18}O diagram (Fig. ~~3c~~4c, grey squares). The isotopic composition of ice wedge IW-28 is also shown in Fig. ~~3a~~ 4a and a clear distinction has to be made between the two different facies of the ice wedge: the ice-sand wedge (ISW-28) and the ice wedge itself (IW-28).~~,~~ These differ both in terms of deuterium-excess (Fig. 4b) ~~(d= δD-8δ^{18}O; Dansgaard, 1964; Figure 3b) a~~and co-isotopic relationship (Fig. ~~3c~~4c). ~~This distinction coincides with a clear visual boundary between the two facies.~~ The ice-sand wedge ISW-28 displays $\delta^{18}O$ values between -29‰ and -30.9‰ and δD values between -230‰ and -246‰. The samples show a low variability in *d* (1σ = ± 0.6‰) with a mean value of 1.4‰, and they are aligned on a slope of 8.03 in the co-isotopic plot. For the ice wedge part IW-28, $\delta^{18}O$ and δD range between -29.4‰ and -31.9‰, and between -229‰ and -247‰, respectively. The *d* also shows a low variability (1σ = ± 0.7‰) with a mean value of 7.5‰ and a slope of 7.44 is measured in the co-isotopic diagram. The transition ~~zone~~ has ~~a~~ $\delta^{18}O$ values between -29.5‰ and -29.9‰, a δD between -223‰ and -237‰, and shows variable *d* values intermediate between the other two parts (Fig. ~~3c~~4c).

4.2. Ice texture and fabrics

Figure ~~4~~ 3 shows thin section photographs that are typical of the three main facies encountered in the two studied ice wedges. In IW-26, the texture is homogeneous, lacking any significant elongation (Fig. ~~4a~~3a). The crystal diameter is ranging between 0.40 and 0.60 cm (10 to 30 mm^2, Fig. 5) and c-axe orientations are concentrated in the horizontal plane with preferred orientation perpendicular to the foliation azimuth (Fig. 6a). The ISW-28 texture shows, within a matrix of relatively large equigranular grains, several monocrystalline layers of elongated crystals with a well-developed “ribbon structure”, and crystal growth being geometrically associated to the fine debris layers that surround them, oriented parallel to the

(subvertical) foliation plane (Fig. 4b). On Fig. 5, crystal diameter is ranging between 0.2 and 0.4 cm (3 to 10 mm^2). In IW-28, the central part of the ice wedge shows an equigranular texture (Fig. 4c), with crystals smaller than in ISW-28 (0.1 to 0.2 cm - 1-3 mm^2, Fig. 5). Both ISW-28 (Fig. 6b) and IW-28 (Fig. 6c) show c-axes orientation patterns similar to IW-26, although the preferred orientation perpendicular to the foliation azimuth is less obvious for ISW-28 given the limited number of observations (due to larger grains).

4.3. Gas properties

The contrast between the three facies (IW-26, ISW-28 and IW-28) is also evident from their gas properties (Fig. 7). Table 1 summarizes minimum, mean and maximum values observed for the ~~3~~ three facies. ~~and compares them to atmospheric pre-industrial and present day values and to meteoric ice range in ice sheets. We highlight that total~~ Total gas contents in our ice wedges are lower than in ice resulting from simple snow compaction as in ice sheets (see ranges in Table 1) and ~~that~~ the total gas content of IW-28 is higher than those of ISW-28 and IW-26. For CO_2, ~~the total~~ all ice wedge mixing ratios are clearly higher than the atmospheric values~~concentrations~~, the highest values being ~~are~~ observed in IW-26 (mean = 62 000 ppmV) and ~~the~~ ISW-28 showing~~s~~ lower values (mean = 3 000 ppmV) than IW-28 (mean = 25 000 ppmV). On the contrary, CH_4 mixing ratios show their lowest values ~~for~~ in IW-26 with values in the ~~same~~ range of ~~the~~ atmospheric mixing ratio ~~concentration~~ (mean = 1 ppmV), ~~high~~intermediate values for IW-28 (mean = 8 ppmV) and ~~very~~ the highest values ~~for~~ in ISW-28 (mean = 55 ppmV). Oxygen shows consistently lower values ~~lower~~ than the atmosphere ~~with values around~~ (of the order of 10%) and nitrogen is slightly higher, balancing other constituents.

4.4. Sediments properties

Residual sediments collected from ~~4~~ four ice samples have been treated with ~~by~~ HCl and H_2O_2 (2 samples from ISW-28 and 2 samples from IW-28). The ISW-28 samples have strongly reacted with H_2O_2 while the IW-28 samples only showed a very limited ~~soft~~ reaction. We therefore argue ~~It can thus be argued~~ that there is organic matter in the ISW-28 sediment inclusions, but only limited amounts in IW-28. On the other hand, the HCl treatment did not show ~~any~~ detectable bubbling activity under the binocular for any of the 4 ~~all~~ sediment samples ~~specimens~~ treated, supporting ~~the hypothesis~~ that carbonate contents are negligible within the sediment enclosed in ~~the~~ our ice wedges.

5 Discussion

In this section, we will first summarize and interpret ice texture and fabrics, co-isotopic signature and gas properties in terms of the infilling process of the studied ice wedges (see also Table 1). We will then attempt to link these processes to the regional paleo-climatic and paleo-environmental setting of the study area.

~~4.5.~~5.1. ~~Ice texture and fabrics~~Ice wedge infilling processes

IW-26

IW-26 is characterized by relatively large grains (Table 1), suggesting either older crystals or conditions favouring recrystallization at higher temperature. The equigranular texture implies no preferred direction of growth (as would be the case for the freezing of a water reservoir) and no significant deformation process. The horizontal girdle of the c-axes with a localized maximum could be explained in several ways: a) gravity settling of individual snow grain in a narrow vertical crack; b) preferential growth along c-axis (better conduction) in a horizontal temperature gradient (perpendicular to crack sides); c) effect of the deformation in wedge during cyclic contractions or d) a combined version between these processes. The spherical bubbles (as opposed to tubular shapes expected in the case of water freezing) also imply no directional freezing, comforting a snow-water mixture hypothesis rather than water infilling for the ice wedge genesis. The total gas content is low in comparison with a dry firn densification process (between one tenth and one third of the value of a dry firnification process) suggesting a liquid water contribution to the ice formation or a process expulsing the gases, eventually along the frost crack if the latter is only partially filled or if the infilling is still permeable.

CO_2 mixing ratios in IW-26 are well above the present-day values (Fig. 7, row 2, left and Table 1). This indicates that the ice did not form through simple low temperature pressure-driven dry firnification process of snow enclosing the atmospheric gas composition. Previous studies of ice forming close to a bedrock environment have shown that this is very often the case, mainly because of either the presence of liquid water and/or significant biological activity within the enclosed organic matter fraction (Souchez et al., 1995a). Theoretically, the high CO_2 solubility in water could raise the CO_2 mixing ratio in the dissolved phase up to about 20 000 ppmV (at 0°C and 1 atmosphere, with limited effect of pressure and impurities).

Freezing of a CO_2 saturated freshwater reservoir in a closed system could therefore display such high CO_2 values. There are however a number of other potential ways to further increase the CO_2 mixing ratio in our ice wedge ice such as diffusion-driven gas fractionation at the freezing front, CO_2 degassing on calcium carbonate precipitation, thermal trapping or biological respiration. Rejection of impurities at the interface by ice growing in a water reservoir will set up a strong diffusion gradient in the adjacent liquid boundary layer. This could lead to a further increase of the mixing ratio of the least diffusive gas in the solution, as for instance CO_2 (Killawee et al., 1998). However, theoretically, this effect cannot increase the CO_2 concentration by a factor higher than the ratio of the CO_2 diffusion coefficient (DCO_2) to the air diffusion coefficient (Dair) in water; i.e. by a factor of about 1.6 (using typical values for DCO_2, DN_2, DO_2). This would increase the CO_2 mixing ratio to about 30 000 ppmV, provided that the freezing process can be assimilated in this case to ice growing in a liquid interface. Killawee et al. (1998) have shown that unidirectional freezing of a supersaturated $CaCO_3$ solution leads to a strong CO_2 enrichment of the refrozen water due to the CO_2 degassing resulting from the carbonate precipitation. The lack of reaction of our ice wedge sediments to an HCl "attack" however does not support the existence of significant amounts of $CaCO_3$. Finally, biological respiration is the most likely active process since bacteria and microbial communities have been identified in permafrost ice and in ice wedges (Gilichinsky et al., 2007; Katayama et al., 2007; Steven et al., 2008).

The considerations above suggest that the CO_2 mixing ratios of IW-26 result from a combination of purely physical processes (solubility) and biological respiration processes. Isotopic measurements of the ^{13}C of CO_2 or of the ^{18}O of the O_2 in our samples would further support this assessment (Cardyn et al., 2007; Souchez et al., 2006), but these data are currently not available. Interestingly though, the range of CO_2 values in the IW-26 ice wedge is similar to that observed in the basal ice of the GRIP ice core (up to 130 000 ppmV), where $\delta^{18}O_{air}$ values as low as -39‰ clearly indicate the occurrence of bacterial respiration processes (Souchez et al., 2006). Tison et al. (1998) and Souchez et al. (1995b), among others, demonstrated that the GRIP basal ice developed under climatically mild pre-ice sheet periglacial conditions. The latter are thus potentially similar to those conditions existing during the formation of our ice wedges. Another approach would be to test for the conservation of the sum of O_2 and CO_2 concentration, given the stoichiometry of the respiration reaction, as suggested by Souchez et al. (1995a). However this approach is not valid in our case since a liquid water phase is present allowing most of the carbon dioxide

produced by the respiration process to dissolve as HCO_3^- into the solution, at least at normal pH levels (Zeebe and Wolf-Gladrow, 2001).

CH_4 mixing ratios are rather low (Fig. 7, row 3, left - Table 1), in the range of Pleistocene – present day atmospheric values and we therefore assume no significant contribution from a substrate source or bacterial production.

The $\delta^{18}O/\delta D$ values in IW-26 are in the range of Late glacial to Holocene ice wedges (Fig. 6b in Wetterich et al., 2011). The slope (6.63) of the linear regression line in the co-isotopic diagram of Fig. 3c is however quite different from the known values of the Local Meteoric Water line in the region (slope of 7.6 at Tiksi Station, H. Meyer, unpublished data). Paleoclimatic interpretation of the stable isotopes signature in ice wedges is usually challenged by the possibility that water phase changes during evaporation/sublimation or melting/refreezing may affect the isotopic composition through fractionation, and therefore potentially alter the original paleoclimatic signature of the ice wedge. Refreezing processes will shift the δ values towards less negative values (e.g., max. +3‰ for $\delta^{18}O$ and +21‰ for δD in a single refreezing process) and will also decrease the slope of the $\delta^{18}O$ - δD co-isotopic relation (Souchez and Lorrain 1991). This is described by the "freezing slope", which is expressed in the more general case of open systems as:

$$S = \frac{\alpha-1}{\beta-1} * \frac{1000+\delta_i D}{1000+\delta_i^{18} O} \quad (1)$$

where $\alpha = 1.0208$ *for deuterium*

$\beta = 1.003$ *for* ^{18}O

δ_i = *isotopic composition of the initial liquid*

This concept has been used by St. Jean et al. (2011) to associate lower co-isotopic slopes to melting-refreezing processes in Holocene ice wedges. It is however important to underline that a "freezing slope" as such will only develop if the scale of the freezing process (size of the water reservoir) is considerably larger than the resolution of the isotopic sampling. In the case of ice wedges, typical crack-widths are of the order of a few centimeters (Harris et al., 1988), and annual "ice veins" are generally observed to be between 1 mm and 1 cm in width. It is therefore quite unlikely to develop a "freezing slope" from a several meters wide ice wedge, using a stable isotopes data set at a resolution of a few centimeters (about 1 cm in our case). This is probably also one of the reasons why $\delta^{18}O/\delta D$ signatures of ice wedges might have paleoclimatic significance. Small-scale refreezing or evaporation/sublimation processes,

if present, are however likely candidates to induce localized small-scale variability towards lower slopes, which might explain the observed lower co-isotopic slope and the lowering of the correlation coefficient ($r^2 = 0.94$) observed in the case of IW-26.

To summarize, our IW-26 analyses enable us to conclude that ice-vein formation in this ice wedge results from refreezing of a water-snow mix, with a large proportion of snow, no directional freezing, although a slight influence of the horizontal temperature gradient on the depositional c-axes orientations might exist. The co-isotopic slope is probably affected by small scale freezing dispersion of the samples. Relatively low gas content and a mixed signature of solubility and respiration processes are also demonstrated for CO_2. These properties are consistent with an ice wedge developing under warm and wet Holocene conditions.

ISW-28

ISW-28 shows medium grains size suggesting less recrystallization and/or younger age than IW-26 (which is actually precluded by the relative stratigraphical position of the two ice wedges, as discussed before). The alternation of equigranular and rectangular crystals (ribbon layer) elongated parallel to the crack side is the main characteristic of the ice-sand wedge part. This type of structure has, to our best knowledge, never been described in ice wedge and resembles the “stratified facies” found in basal glacier ice (e.g. Tsijiore Nouve, Switzerland) or ice resulting from film water refreezing on subglacial cavity floors. In our case we assume interface freezing on the cold surface of the frost crack walls of a thin running water film originating from summer melting of the surface lips of the partially open (unfilled) crack (as opposed to a “top-down” or “side-center” refreezing of an “in situ” bulk water reservoir). Sediments at layer boundaries suggest entrainment with the melt water from the surface, rejection from the growing ice and, finally, freeze-in during “shut-down” phases of the water supply. The horizontal girdle drawn by the c-axes distribution does not show a localized maximum, but, as mentioned before, the number of sample is relatively low. The observed high small-scale variability of total gas content is probably due to the alternation of layer with bubbles (episodes of wet snow metamorphism) and layers without (ribbon layer formed through water film freezing). CO_2 is higher than atmospheric values (solubility effect) but well below solubility limit of 20 000 ppm, therefore suggesting an “open system” freezing with gas rejection to atmosphere. CH_4 mixing ratios are much higher than the atmospheric value, suggesting methane production in bubbles or in soil, in close vicinity to the bubbles

before their occlusion in the ice vein. Note that the sediments in the ice-sand wedge part are rich in organic matter and provide an adequate substrate for methanogenic bacteria.

Methane production implies an anaerobic environment for the methanogenic archaea to work efficiently (e.g. Wagner and Liebner, 2009). Although ice wedges can be a source of methane (e.g. Meyer et al., 2010a), the range of observed methane mixing ratios seems to be negligible compared to other methane sources studied for the carbon budgets in permafrost area (IPCC, 2007). Apart from a few values close to atmospheric in ISW-28, the O_2 mixing ratio fluctuates around 10% (Fig. 7, row 4), being only half the atmospheric O_2 value. It is hard to tell if this value is the gaseous composition of the local environment (in the crack into the frozen soil) before the bubbles "close-off" or if this value is a result of biogeochemical post-occlusion processes. Whichever way, it does not imply a fully anaerobic environment. However, for O_2 measurements only ±35 g of samples were taken, each containing a large number of millimetric bubbles. As already suggested for the GRIP basal ice (where both high CO_2 and high CH_4 values were measured in the same samples) and in other environments like soils and marine sediments (Souchez et al., 1995b), the mean O_2 concentration might well reflect a situation where some bubbles are depleted in oxygen and others have concentrations close to atmospheric levels. The bubbles can therefore provide contrasted closed system micro-environments in some cases favourable to aerobic respiration (high CO_2, low CH_4) and in others to bacterially mediated methanogenesis (high CH_4, low CO_2).

The $\delta^{18}O$ and δD values match well with Pleistocene stadial signature in the studied area (Fig. 6c in Wetterich et al., 2011). The slope in the co-isotopic diagram (8.03) could be indicative for the variability of the autumn – winter snow input to the crack during the integrated period of the ice-sand wedge history. Snow samples in this region do not receive additional secondary moisture (because open water bodies are frozen in winter) and therefore are generally situated close to the GMWL (Meyer et al., 2002a, 2002b) with slopes in the co-isotopic diagram close to 8.

ISW-28 ice veins properties suggest a mixed origin altering episodes of consolidation of a "water-snow" mix (granular) and of events of running water film refreezing at the sides of the open frost crack. The fact that the crack is not always filled with snow might indicate periods favouring debris incorporation either through an increased input of particulate contribution from the surface or because of a thinner snow cover (lower precipitations). It is worth noting that a globally colder-drier period (as suggested by the low precipitation) does not necessarily mean less melting in the period when frost cracks are open, if debris availability allows strong

summer albedo effects. The biological activity in ISW-28 is characterized by low to moderate aerobic respiration but high methanogenic activity related to availability of organic matter and lower than atmospheric oxygen levels. These conditions obviously existed during the early stages of IW-28 development (ISW-28).

IW-28

IW-28 shows the smallest grain size. This is potentially the combined result of a lower Arrhenius growth rate at lower temperature and less liquid water availability (which would otherwise enhance crystal growth rate). Clearly these factors took over the "time factor" (older ice) in the recrystallization process. The equigranular ice does not show preferred direction of freezing and the horizontal girdle shows one localized maximum sub-perpendicular to the foliation, as for the IW-26. As in IW-26 also, the spherical bubbles indicate no directional freezing and favour a consolidation process of a snow-water mixture for the origin of the ice veins. However, the highest total gas content with values reaching about 50% of those observed in dry firnification), suggest less liquid water contribution than in IW-26. This might be linked to the small-scale hydrodynamical processes at play as the meltwater percolates into the snow infilling. Colder temperatures in the surface permafrost from the previous winter would favour rapid freezing in the surface layer and limit water percolation further down-crack. Detailed vertical gas content profiles would certainly be useful in documenting these processes further.

CO_2 mixing ratios contrast with those observed in the ISW-28 section and are closer to those observed in ice wedge IW-26, showing the potential combination of pure physical solubility processes with biological respiration, although the latter is less developed than in IW-26. CH_4 mixing ratio, largely higher than the atmospheric values, are also intermediate between those of IW-26 and ISW-28. $\delta^{18}O$ and δD values are similarly low as compared to ISW-28 and might suggest a slightly colder period for IW-28.

IW-28 should therefore be formed from a water-snow mix, at relatively low temperature than IW-26, with a large proportion of snow, no directional freezing and less sediments input than in ISW-28. The latter results in moderate CH_4 mixing ratios, although these are higher than those measured in the Holocene ice wedge IW-26. Fabrics are still dominated by horizontal c-axes including a single maximum roughly perpendicular to the crack sides, suggesting gravity settling control or contraction deformation effects rather than recrystallization growth, given the isotropy of the bubbles and crystal shapes.

Our interpretation of ice wedge filling process and ice vein formation contrasts with St-Jean et al. (2011) which suggest that the Holocene ice wedges result from the freezing of liquid water and that the Pleistocene ice wedges result rather from snow densification and/or hoarfrost accretion. Our study suggests variable water-snow mix as source of the ice with higher water contribution during the Holocene period. Coherently with Lacelle et al. (2011) and St-Jean et al. (2011) data, however, our $\delta(N_2/Ar)$ and $\delta(O_2/Ar)$ results (Fig. 8) indicate an increasing influence of biological processes with the increasing amount of water in the water-snow mix. Interestingly, the proximity of the debris source could result in a larger proportion of melting as compared to the snow matrix, and enhanced methanogenesis even though the climate is colder. The latter is supported by a study of Meyer et al. (2010a) in Northern Alaska, where an ice wedge component formed during the colder Younger Dryas displays higher methane concentrations as compared to an ice wedge section formed during the warmer Allerød. Clearly, environmental, physical and biological controls need to be considered when discussing ice wedge properties.~~Crystal size and shape provide information about ice formation (e.g. Paterson, 1994). Ice wedge IW-26 is clearly younger than IW-28 as indicated by its stratigraphic location within the cliff. IW-26 does not show variations in crystal size from the centre to the border (Fig. 5). There are however some arguments in favour of such variations in IW-28 (note the V-shape of the curve to the right of the ice-sand wedge, Fig. 5). It is unlikely that the larger crystal size (e.g. in IW-26) predominantly results from seasonal deformation. Indeed, crystal size is fairly homogeneous throughout the ice wedge and there is no evidence of structural features (folds, shears planes, etc.) that would be generated by seasonal ice-wedge contraction. Finally, the absence of ongoing deformation is further supported by the horizontal c-axes orientations (Black, 1954, 1963, 1976; Corte, 1962; Gell, 1976) and the absence of strain shadow within individual crystals. This suggests that the primary controls on the crystal size in IW-26 are temperature and possibly increased water infiltration, which would be consistent with an ice wedge developed under Holocene conditions.~~

~~ISW-28 shows a peculiar "ribbon-like" structure embedded into a matrix of equigranular crystals. This type of structureresembles those found in the "stratified facies" found in basal glacier ice (Knight, 1999; Lawson, 2007; Samyn et al., 2005). In this environment, this mono-crystalline ice layer "sandwiched" between two fine debris layers was likely formed as a result of recrystallization in an environment of liquid water streaming, generally as a thin film, at the ice bedrock interface and refreezing on the lee side of bedrock irregularities. These~~

observations suggest liquid water occurrence during the ice-sand wedge formation. Debris incorporation resulted from particular surface conditions and specific mineral and/or water supply such as an increased part of surface matter content, or a thinner snow cover. These conditions obviously existed during the early stages of IW-28 development. We therefore assume that ice in ISW-28 was formed within different environmental conditions than ice in IW-28. The crystals in the latter are smaller and show an equigranular texture; crystal growth mechanisms were therefore probably slower in this debris-poor ice, suggesting potentially colder ice.

4.6. Gas properties

Gases analyses (Fig. 7) further support the conclusions drawn from the ice texture description. All samples display a low total gas content (Fig. 7, row 1) in comparison with meteoric glacier ice formed under dry conditions. We hypothesize that these low values are due to liquid water infiltration during the ice wedge formation. Indeed, bubble density, geometry and distribution (Fig. 4d) suggest that the studied wedge ice originated from a mixture of snow and water filling thermal contraction cracks in variable amount, rather than solely from snow compaction. Especially since it has been observed that water standing in the apex (above the crack) enters the crack at once. That is also why the mean isotopic composition of recent ice wedges often corresponds to that of snow. In these conditions, total gas content should follow an inverse relation to the liquid water content. The liquid water contribution is apparently larger for IW-26 than for IW-28. This is consistent with a colder environment for IW-28 also confirmed by the isotopic composition. Another characteristic feature of ISW-28 is that its gas content is alternating between very low values, down to about 10 $ml_{air}kg^{-1}_{ice}$ (the lowest in this study), and values intermediary between those of IW-26 and IW-28. This is the expected signature for alternation of episodes of film water refreezing as “ribbon layers” (low total gas content) incorporating sediments at the beginning and at the end of the refreezing process (phases of interruption of film waterflow), with an equigranular matrix corresponding more to wet snow consolidation (higher total gas content). Another potential explanation would be that the ribbon layers are due to the freezing of a water body from the rim of the crack towards its centre and the associated entrainment of particles, ions and gas bubbles. However, this would result in bubbles inclusions elongated perpendicular to the freezing front direction which are not detected here.

~~All CO_2 mixing ratios are largely above the present day atmospheric value of 390 ppmV (Fig. 7, row 2). This indicates that the ice did not form through simple low temperature pressure-driven dry firnification process of snow enclosing the atmospheric gas composition. Previous studies of ice forming close to a bedrock environment have shown that this is very often the case, mainly because of either the presence of liquid water and/or significant biological activity living on the enclosed organic matter fraction (Souchez et al., 1995a). Theoretically, the high CO_2 solubility in water could raise the CO_2 mixing ratio in the dissolved phase up to about 20 000 ppmV (at 0°C and 1 atmosphere, with limited effect of pressure and impurities). Freezing of a CO_2 saturated freshwater reservoir in a closed system could therefore display such high CO_2 values. There are however a number of other potential ways to further increase the CO_2 mixing ratio in our ice wedge ice such as diffusion driven gas fractionation at the freezing front, CO_2 degassing on calcium carbonate precipitation, thermal trapping or biological respiration. Solutes segregation as observed ahead of a freezing front, rejection of impurities at the interface by ice growing in a water reservoir will set up a strong diffusion gradient in the adjacent liquid boundary layer. This could lead to a further increase of the mixing ratio of the least diffusive gas in the solution, as for instance CO_2 (Killawee et al., 1998). However, theoretically, this effect cannot increase the CO_2 concentration by a factor higher than the ratio of the CO_2 diffusion coefficient (DCO_2) to the air diffusion coefficient (Dair) in water; i.e. by a factor of about 1.6 (using typical values for DCO_2, DN_2, DO_2). This would increase the CO_2 mixing ratio to about 30 000 ppmV, provided that freezing process can be assimilated in this case to ice growing in a liquid interface. Killawee et al. (1998) have shown that unidirectional freezing of a supersaturated $CaCO_3$ solution leads to a strong CO_2 enrichment of the refrozen water due to the CO_2 degassing resulting from the carbonate precipitation. The lack of reaction of our ice wedge sediments to HCl attack however does not support the existence of significant amount of $CaCO_3$. Finally, biological respiration is also a likely candidate, given a similar behaviour of our samples compared to segregated ice (Cardyn et al., 2007).~~

~~The considerations above suggest that the CO_2 mixing ratio of IW-26 (40 000-100 000 ppmV) is dominated by biological respiration processes while IW-28 CO_2 levels could still be fully explained by physical processes alone (although biological processes cannot be excluded). Isotopic measurements of the ^{13}C of CO_2 or of the ^{18}O of the O_2 in our samples would further support this assessment (Cardyn et al., 2007; Souchez et al., 2006), but these data are currently not available. Interestingly though, the range of CO_2 values in the IW-26 ice~~

wedge is similar to that observed in the basal ice of the GRIP ice core (up to 130 000 ppmV), where $\delta^{18}O_{air}$ values as low as -39‰ clearly indicate the occurrence of bacterial respiration processes (Souchez et al., 2006). Tison et al. (1998) and Souchez et al. (1995b), among others, demonstrated that the GRIP basal ice developed under climatically mild pre-ice sheet periglacial conditions. The latter are thus potentially similar to those surrounding our ice-wedge samples. Another approach would be to test for the conservation of the sum of O_2 and CO_2 concentration, given the stoichiometry of the respiration reaction, as suggested by Souchez et al. (1995a). However this approach is not valid in our case since a liquid water phase is present allowing most of the carbon dioxide produced by the respiration process to dissolve as HCO_3^- into the solution, at least at normal pH levels (Zeebe and Wolf-Gladrow, 2001). There is also a clear contrast between the CO_2 concentrations of most of the ISW-28 samples as compared to those of IW-28. This contrast could reflect differences in the ice-wedge formation process. The CO_2 levels close to maximum solubility in IW-28 suggest limited exchange with the atmosphere and the reverse is valid for ISW-28, as also demonstrated by the contrast in total gas content. This supports the hypothesis of a contrasting dynamic between the genesis of the ribbon facies of ISW-28, the geometry of which suggesting higher temperature allowing recrystallization and/or open-system growth from a running water film, and of the ice within the central part of ice wedge IW-28, which results from bulk refreezing of a mixture of snow and interstitial water.

Methane also displays strong contrasts between the three ice-wedges facies, with a general inverse relation to the CO_2 concentration (Fig. 7, row 2 and 3). While IW-26 concentrations range between pre-industrial and present day values, IW-28 and ISW-28 are by a respective factor of 10 to 100 higher suggesting *in situ* CH_4 production. Methane production implies an anaerobic environment for the methanogenic archaea to work efficiently (e.g. Wagner and Liebner, 2009). Although ice wedges can be a source of methane production, the range of methane content observed seems to be negligible in regard with other methane sources studied for the carbon budgets in permafrost area (IPCC, 2007). Apart from a few values close to atmospheric in ISW-28, the O_2 concentration fluctuates around 10% (Fig. 7, row 4). It is only half the atmospheric O_2 mixing ratio and it is hard to tell if this value is the gaseous composition of the local environment (in the crack into the frozen soil) before the bubbles close off or if this value is the result of biogeochemical post-genetic processes. Whichever way, it does not imply a fully anaerobic environment. However, one must recall that the measurements were taken from ±35 g samples each containing a large number of millimetric

~~bubbles. As already suggested for the GRIP basal ice (where both high CO_2 and high CH_4 values were measured in the same samples) and in other environments like soils and marine sediments (Souchez et al., 1995b), the mean O_2 concentration might well reflect a situation where some bubbles are depleted in oxygen and others have concentrations close to atmospheric levels. The bubbles can therefore provide contrasted closed system micro-environments in some cases favourable to aerobic respiration (high CO_2, low CH_4) and in others to bacterially mediated methanogenesis (high CH_4, low CO_2). Note that the contrast in this CO_2/CH_4 relation is mainly between ice wedges, rather than within a given ice wedge. Brouchkov and Fukuda (2002) also observed an inverse correlation between CH_4 and CO_2 in ice wedges. Their study reveals an important CH_4 mixing ratio variability (2 to 6 000 ppmV), which they attributed to the contrasted vegetation cover, which, in their case, consist of a forest that increase methane production.~~

~~The methane concentration of the ice-sand wedge ISW-28 contrasts with the central part of IW-28 displaying highest CH_4 levels in the ice-sand wedge whereas anaerobic conditions are somewhat less pronounced. This could be the expression of a higher availability of organic substrates in the debris-rich ice-sand wedge. This hypothesis is supported by the obviously positive reaction of H_2O_2 with the residual sediments from ISW-28. From the above discussion it is clear that both environmental, physical and biological controls need to be taken into account to interpret the observed gas properties in ice wedges. As demonstrated by the comparison between IW-26 and IW-28, it is not always when the temperatures are warmer that the highest CH_4 concentration levels are observed. This is supported by an ice wedge study of Meyer et al. (2010a) in Northern Alaska, where an ice-wedge component formed during the colder Younger Dryas displays higher methane concentrations as compared to an ice wedge section formed during the warmer Allerød. Thus, the availability of organic matter within the deposits (as in ISW-28) and in semi-closed system conditions might favour methanogenesis and limit CH_4 conversion to CO_2.~~

~~4.7.~~5.2. Links to the regional paleoclimatic interpretation ~~$\delta^{18}O$ – δD isotopic composition of ice wedges~~

Results from texture, fabric and gas analyses allow to differentiate between three ~~different~~ facies within the two studied~~s~~ ice wedges (IW-26, ISW-28 and IW-28), which can also be discussed in terms of the regional paleoclimatic interpretation from available stable isotopes data.~~available stable isotope data.~~

The IW-26 displays least negative δD and $\delta^{18}O$ values, largest crystal sizes, lowest total gas contents and is embedded in the Ice Complex structure of Pleistocene age. However, ~~the~~ its isotopic composition is coherent with Holocene age ice wedges ($\delta^{18}O$ around -24 to -25‰; Meyer et al., 2000, 2002a, 2002b; Dereviagin et al., 2002; Schirrmeister et al., 2002; Popp et al., 2006; Meyer et al., 2010b) ~~($\delta^{18}O$ around -24 to -25‰; Meyer et al. 2000, 2002a, 2002b; Dereviagin et al. 2002; Schirrmeister et al. 2002; Popp et al. 2006; Wetterich et al. 2008). We therefore attribute this ice wedge to the Holocene.~~ A period of mild temperatures would also increase the rate of biological respiration processes and the availability of organic matter. ~~Note that the IW-26 samples plot on a slope of 6.63±0.15 in the co-isotopic diagram of Fig. 3c, which deviates from the LMWL – slope of 7.6 (Tiksi; Meyer, unpublished data). Paleoclimatic interpretation of the stable isotopes signature in ice wedges is usually challenged by the fact that phase changes such as evaporation or melting and refreezing are known to affect isotopic ratios through fractionation and therefore potentially alter the original paleoclimatic signature of the deposit. Refreezing processes will shift the δ values towards less negative values (e.g., max. +3‰ for $\delta^{18}O$ and +21‰ for δD in a single refreezing process) and will also decrease the slope of the $\delta^{18}O$ – δD co-isotopic relation (Souchez and Lorrain 1991). This is described by the "freezing slope", which is expressed in the more general case of open systems as:~~

~~$$S = \frac{\alpha - 1}{\beta - 1} * \frac{1000 + \delta_i D}{1000 + \delta_i^{18} O} \quad (1)$$~~

~~where α = 1.0208 for deuterium~~

~~β = 1.003 for ^{18}O~~

~~δ_i = isotopic composition of the initial liquid~~

~~Evaporation/sublimation processes or small scale refreezing processes (the calculated freezing slope would be 5.79 ±0.02, using Eq. (1) and the mean IW-26 δ values) are 2 possible assumptions to explain the observed slope. Both alternatives would equally be favoured under relatively warm conditions, as hypothesised above.~~

The lower isotopic composition of IW-28 suggests a Pleistocene origin (compare Fig. 6b of the recent regional overview in Wetterich et al. (2011). ~~($\delta^{18}O$ around -30‰). Although,~~ T~~t~~he situation is ~~probably~~ however certainly more complex for the ISW-28/IW-28 case as ~~displayed~~ suggested by ~~a clear~~the strong contrast in their *d* values, ~~showing~~ while showing in both cases low internal variability ~~, of ISW-28~~ (mean d= 1.4‰ for ISW-28 and mean d=7.5‰

for IW-28) ~~and IW-28 (mean =7.5‰),~~ for similar δD ranges (Fig. 4~~3~~). Also worth noting is the sharp monotonic transition in *d* values at the interface between ISW-28 and IW-28.

There is a number of ways to explain low *d* in precipitations (and in the ice that evolves from it), that either belong to the "water cycle processes" or to the "*in-situ* post-deposition processes". Extensive work has been done dealing with the concept and use of ~~the~~ *d* in co-isotopic studies, especially in the field of deep ice-~~-~~core interpretation and the relation to temperature changes at precipitation sites and oceanic sources (Craig, 1961; Dansgaard, 1964; Merlivat and Jouzel, 1979; Yurtsever and Gat, 1981; Jouzel et al., 1982, 2005a, 2005b; Jouzel and Merlivat, 1984; Johnsen et al., 1989; Masson-Delmotte et al., 2005; Stenni et al., 2001, 2004; Vimeux et al., 2002, 1999). It is commonly admitted that, although humidity and wind speed at the source also play a role, in most cases, the $\delta^{18}O_{ice}$ and δD_{ice} primarily depends on the temperature at the site (T_{site}) and to a lesser extent on the temperature at the source (T_{source}). The reverse is true for the *d* in the ice. The latter is indeed mainly driven by kinetic isotopic effects during evaporation at the oceanic source, and these will be enhanced for higher temperatures and lower relative humidity, increasing the *d* value (Masson-Delmotte et al., 2005; Merlivat and Jouzel, 1979). It should however be kept in mind that at equivalent source temperatures, lower winds would also increase the relative humidity at the source and therefore decrease the d-excess. As shown in the deep ice core records from Greenland, large topographic ~~During the last glacial period (Dansgaard-Oeschger events), large topographic~~ and atmospheric circulation changes during the last glacial period (the presence of ice sheets of variable size, larger but fluctuating extension of the sea ice) are ~~also~~ responsible for an antiphase relationship between δ values (T_{site}) and *d* values (T_{source}). Indeed, during mild events, when Greenland was warmer (less negative δ's) and ~~the~~ sea ice ~~extension lower~~less extent, the moisture source was closer (colder) and therefore the *d* lower ~~and vice-versa~~than during more severe phases. This results in the samples from these milder periods ~~can explain the fact that the samples from these milder periods~~ (less negative δD and $\delta^{18}O$) ~~are aligned~~ aligning, in a δD-$\delta^{18}O$ diagram, on a line with slope close to 8, but with the d-intercept at ~~on a line with slope close to 8, but with a d-intercept of~~ +4‰ instead of +8‰ (e.g. Fig 7 in Johnsen et al., 1989)~~(e.g. Fig 7 in Johnsen et al., 1989)~~.

Today, t~~T~~he main source of the winter precipitation in our study area (west of ~140°E) ~~today~~ is probably located in the Northern Atlantic (Kuznetsova, 1998; Rinke et al., 1999). However, as discussed by Meyer et al. (2002b) and Wetterich et al. (2011), Pleistocene moisture sources

for the same area less straightforward to locate. Two hypotheses were discussed (Table 2): (1) refers to a permanent Atlantic source, with a latitudinal variation similar to that suggested by Johnsen et al. (1989), as described above for Greenland. In that scenario, a contrasting *d* signature would represent a temporal shift (within the Pleistocene, e.g. interstadial/stadial) from a milder (Table 2, col. 2) glacial period (higher T_{site}) with a higher relative humidity ~~are more difficult to locate, nevertheless, Meyer et al. (2002b) have already discussed two possible hypotheses. The first one is the Atlantic with the latitudinal variation due to the ice area variation suggested by Johnsen and White (1989). The second one discusses about the potential variations of atmospheric moisture circulation due to the Eurasian ice sheet extension enabling a contribution from the Northern Pacific which is known to have a lower *d*. Meyer et al. (2010b) already have identified sources moisture variation during the Younger Dryas in Northern Alaska. In our case, the *d* shift between ISW-28 and IW-28 occurred during the Pleistocene, suggesting the contrasting δD-$\delta^{18}O$ signature of our coastal ice wedge ISW-28/IW-28 could represent a shift from a milder glacial period with a more proximal ocean source (due to a lesser sea ice cover) at a lower temperature~~ (i.e. lower T_{source} and/or lower winds, and therefore~~,~~ lower *d* values in ISW-28) to a colder glacial period (lower T_{site}) with a lower relative humidity ~~more distal ocean source at a higher temperature~~ (i.e. higher T_{source}, and/or higher winds, and therefore higher *d* value in IW-28). The amount of precipitation, however, should be lower during cold stadial periods and higher during interstadials (as for the difference between glacials and interglacials in deep ice cores and in permafrost).~~–~~Alternatively, (2) the combination of the full development of the Eurasian Ice Sheet (the easternmost extent of which reached the western part of Taymyr Peninsula) and of an extended sea ice cover in the Barents and Kara seas and the Northern Atlantic (stadial, Table 2, col. 5), might have considerably reduced (deflected or even blocked Meyer et al., 2002a) the penetration of Atlantic air masses to the Laptev Sea region. In that case, a stronger influence of the North Pacific winter moisture source, with low *d* values and low precipitation (e.g. Clark and Fritz, 1997), could have existed. Note however that the occurrence of this specific North Pacific moisture low *d* isotopic signature east of our study site is still somewhat controversial in ground ice (Schwamborn et al., 2006). During interstadials (Table 2, col. 4), on the contrary, a distinct Northern Atlantic source could have been re-established, with potentially higher *d* values (more "southerly" sources) and higher precipitation (Lacelle et al., 2011). We will discuss below these two alternatives, in the light of the other ice properties.

Climatic seasonal variations (temperature, precipitation, etc.) are also able to disturb *d* ~~On the other hand, a radical modification of the source origin should be unlikely to explain this *d* shift without showing a clear gap in the isotopic profile. Climatic seasonal variations (temperature, precipitation, etc.) are also known to be able to disrupt *d*~~ (Johnsen et al., 1989; Meyer et al., 2002b) but ice wedges are known to be built from the winter snow precipitation mainly and the spring meltwater derived from it. ~~, therefore, it is delicate to discuss this hypothesis although earlier precipitations in Autumn with a lower *d* could be an explanation.~~

Post-depositional "*in situ*" phase changes could also be responsible for lowering the *d* values of the samples (Meyer et al., 2002b). Isotopic fractionation during ice wedge consolidation was discounted by ~~can be discarded according to~~ Michel (1982) based upon the argument that freezing is generally too fast to allow for ~~fractionation~~it. However, conditions might be different for the formation of the "ribbon facies" ~~of~~ in the ice-sand wedge for example. Figure ~~8~~ 9 shows the effect of equilibrium fractionation during hypothetical 10% refreezing (grey squares) of water resulting from the melting of each of the samples from IW-28 (black dots). The mean isotopic composition of the 10% refrozen fraction was computed using the formulation in Souchez and Lorrain (1991) as in Eq. (2), with a frozen fraction (K)=0.10.

$$\bar{\delta}_s = 10 * (1000 + \delta_0) * [(1.1 - K)^{\alpha} - (1 - K)^{\alpha}] - 1000 \qquad (2)$$

where $\bar{\delta}_s$= *δ value of refrozen samples*

δ_0 = *δ value of water (melted IW-28 ice sample, no fractionation on melting* (Moser and Stichler, 1980; Souchez and Lorrain, 1991)*)*

K = frozen fraction

α = *fractionation coefficient (1.0208 for deuterium and 1.003 for* ^{18}O*)*

The ~~modelled~~ refrozen IW-28 samples indeed reproduce the *d* of the ISW-28 samples and lie on ~~using K=10 reproduce the *d* of the ISW-28 samples and lie on~~ the same co-isotopic line. They are however clearly offset towards less negative δ values, and more negative *δ* values than observed in IW-28 would be required to explain the observed ISW-28 *δ*-range. This is not precluded, given the existence of some more negative values from the Sartan period reported by e.g. Wetterich et al. (2011, Fig. 6) in other ice wedges of the area. Experimental sublimation/evaporation processes of a snow pack have also been shown to shift the remaining reservoir towards less negative isotopic values with a slope that is less than 8 (Souchez and Lorrain, 1991 and references within). ~~Submitting the IW-28 samples to such a~~

~~fractionation process would also shift their *d* towards lower values.~~ However, although they could reproduce the observed *d* values in ISW-28, both of these post-depositional processes would need to be occurring at a rigorous equivalent rate (e.g., 10% refreezing, fixed evaporation percentage) for all samples to plot on a co-isotopic line as well defined as the one observed for the ISW-28 samples, with a slope close to 8. ~~As a matter of~~In fact, the very good alignment of all the ISW-28 samples on a line with a slope of 8.03 (r^2=0.98, with a fairly low range of the δ values) is ~~in itself~~ an argument to favour a "classical" Rayleigh-type "source to sink" fractionation history.

This leaves us therefore with the first hypothesis of a major shift ~~southward~~ in the moisture source (higher *d*), as the ice wedge growth switches from ISW-28 to IW-28, across the transition ~~zone~~. Do the other ice properties allow us to decipher between the two alternative moisture source changes, with opposite conclusions in terms of the *d* signature? The answer is not straightforward. Indeed, ISW-28 has very low d-values (Table 2, col. 6 and Fig. 4) which would either correspond to an interstadial period in hypothesis 1 (Atlantic source, little sea ice cover - Table 2, col. 2) or to a stadial in hypothesis 2 (North Pacific source - Table 2, col. 5). The latter option is coherent with the deduced lower relative precipitation amounts from the observation of the ice-vein properties at ISW-28. However, in that case, the "in-situ" temperature should be lower at ISW-28 than at IW-28 (which would then be typical of re-establishment of an Atlantic source with higher d-values and higher precipitation). Alternatively, higher T_{site} for ISW-28 fit to an interstadial in hypothesis 1 (change in position of Atlantic source), but then higher precipitation amounts should be expected (Table 2, col. 2). Note however that the δ-contrast is low between ISW-28 and IW-28, and that it should also be strong if hypothesis 1 was valid, with much higher values for ISW-28, provided that the mechanism is similar to the one presented for the Greenland Ice Sheet "stadial-interstadial" alternation by Johnsen et al., 1989. The latter assumption is hypothetical. Indeed, precipitation and temperature regimes on the downwind side of major ice-sheets might have been quite different to those existing in its centre parts (e.g. foehn effects which would locally increase temperatures and lower precipitations). One could also argue that the "switch" from North Pacific to Atlantic sources in hypothesis 2 could also be primarily linked to changes in the Greenland and Eurasian Ice Sheets geometries, which might in turn not be directly linked to contrasted global temperature regimes but to other mechanisms such as ice-ocean interactions.

In the ISW-28 ice-sand wedge the dominance of debris input over snow filling, suggests a period of limited precipitation in accordance with the North Pacific winter moisture source with a low *d* value. However, the thin sections suggest the presence of meltwater and of melting-refreezing processes in an open-system, sandwiched with refrozen snow layers of limited extension (also supported by the total gas content measurements). Intuitively, these would be preferably associated to warmer periods, but they could also simply result from albedo effects in this debris-rich environment.

~~There is, however, an apparent discrepancy with similar cases in ice-core records (for example, shifts from mild to cold glacial periods as described in Fig. 7 of Johnsen et al. (1989)), where an increase in the *d* value is always accompanied by a shift of both the δD and $\delta^{18}O$ values towards colder, more negative values (and vice-versa). This is less clear in the data of Fig. 3. Although the range of $\delta^{18}O$ values can reasonably be considered as "colder" in IW-28. This might be understandable for moderate coolings, since an increase in T_{source} will kinetically affect $\delta^{18}O$ more than δD. It seems also somewhat straightforward that the amplitude of changes in δ values between milder and colder event during the Pleistocene would be smaller closer to sea level than in the central part of the Greenland Ice Sheet. The relative contribution of T_{source} and T_{site} to the δ's signatures could also be different at coastal sites, but that would require model simulations for testing. Aside from the potential sources variation, the ice-sand wedge facies results from a local environment change with probably a thinner snow cover or an earlier cracks opening (before the snow cover presence) to enable the particles to be blown/entrained into the cracks. A very thin snow cover could change the local albedo by allowing the accumulation of particles on the snow, supporting more water streaming which should contribute to the formation of the "ribbon facies". A very thin snow cover might also suggest an important local role of sublimation and evaporation processes with potential post-depositional impact on the d-value, as suggested above. Although a constant sublimation rate needs to be invoked to explain the observed strict alignment of the samples along the co-isotopic slope, this hypothesis cannot be ruled out.~~

~~Regardless of the fact that both variation of local conditions and T_{source} modification might explain the *d* shift between ISW-28 and IW-28, in both cases the ISW-28 section reflects a climate characterized by milder temperatures, more important liquid water contribution to the ice genesis and a time period in the year with a very thin snow cover and access for the particles to the inner crack.~~

~~5~~6 Conclusions

~~We analyzed 2 ice wedges (IW-26 and IW-28) from a cliff located in Arctic Siberia, in order to understand the specific conditions of their formation process.~~ Detailed crystallographic, gas content and composition, and water isotope analyses of the IW-26 and IW-28 ice wedges allowed us to shed more light on the processes involved in ice wedge growth. ~~Our multi-parametric approach suggest that water isotopes can be used locally as reliable climate indicators and that the studied ice wedges formed under different environmental conditions. The i~~Ice wedge IW-26 ~~is found to have~~has developed in a mild Holocene environment. Higher temperatures and higher meltwater infiltration resulted in enhanced recrystallization, larger crystal sizes, lower total gas content and favourable conditions for biological respiration, inducing relatively high CO_2 levels. Ice wedge ISW-28/IW-28 ~~was initiated~~developed in a relatively mild Pleistocene environment, during which a large change in atmospheric sources occurred, as documented by a sharp monotonous transition in deuterium excess from stable values at ca. 1.4‰ in ISW-28 (early growth) to stable values at ca. 7.5‰ in IW-28, that cannot be explained through post-depositional processes. This transition occurred without significant changes in the site temperature as indicated by constantly low $\delta^{18}O$ and δD values. It is however difficult to select potential mechanisms behind the changes in atmospheric sources. The transition is however concurrent with major changes in the ice wedge morphology. The ice-sand wedge ISW-28 properties show a smaller contribution of refrozen "snow-water mix" in the ice veins, with regular episodes of film water open-system refreezing on the crack walls, associated with important losses of total gas content and abundance of surface-derived debris inclusions forming the "ribbon facies". This heterogeneous medium, rich in organic matter, might have favoured the anaerobic micro-environmental conditions necessary to explain the maximum CH_4 levels in that unit. Ice veins texture in IW-28 resemble more the refrozen "snow-water mix" of IW-26, but with smaller crystal sizes and larger total gas content, as would be expected from colder conditions.

The changes in *d* between ISW-28 and IW-28 are most likely linked with changes in the moisture source region from Atlantic to Pacific or changes within an Atlantic source region. The combined observed low *d* values and limited snow contribution to the ice vein matrix, suggesting low precipitation, in ISW-28 is consistent with a North Pacific atmospheric source for the local precipitation at the time of ISW-28 formation. The length and persistence of this low *d* event is however unknown since it has not been observed at any other ice wedge study

site west of 130°E. The significant contrast in ice veins metamorphic processes between ISW-28 and IW-28, suggesting a larger contribution of melting-refreezing processes in the former, could result from slightly milder conditions at ISW-28. However, the close proximity of the soil-sediment source has certainly fostered melting through albedo feedbacks.

Finally, comparing our methane mixing ratios in IW-26 and IW-28 reveals that substrate availability is as important as the temperature regime in controlling production rates in the permafrost environment.~~probably characterized by a moisture source with comparatively higher relative humidity, as revealed by the uniformly low *d* value in ISW-28. The local conditions at the time of formation were probably warmer than later on, favouring meltwater production in an environment characterized by periods of limited amount of snow and close proximity to a soil/sediment source, eventually further fostering melting through the albedo feedback. These conditions led to the typical "ribbon" layer texture. We interpret the low total gas content in the "ribbon" layers and the higher values in the surrounding equigranular texture as resulting from the freezing of a thin meltwater film running on the open frost crack of the ice wedge partially filled with snow. This heterogeneous medium, rich in organic matter, might have favoured the anaerobic microenvironmental conditions necessary to explain the maximum CH_4 levels in that unit. The analysis of *d* values further allowed constraining the local climatic conditions. As the climate started to cool, a transition occurred in the central part of the IW-28 ice wedge, as documented by the higher *d* values documenting in this part, suggesting a synchronous major change in the moisture source for the snow falls towards a more meridional ocean source. As suggested by several authors discussing the Greenland Pleistocene ice-core records, this might reflect the switch towards larger ice sheets and/or sea ice extents. These cooler conditions limited crystal size growth, total gas loss, biological respiration activities and CH_4 production, although the latter might also have been influenced by the unavailability of organic substrate. It should be noted that the system apparently never returned to milder climatic conditions before the ice wedge ceased being active, suggesting that its lifetime spanned a few thousand years at the most.~~

Acknowledgements

We thank all participants of the Russian-German expedition "Lena Anabar 2003". Sampling and analytical work in the AWI Potsdam laboratories was supported by Antje Eulenburg,

Eileen Nebel, Ute Bastian and Lutz Schönicke. This study is part of the Russian-German cooperative scientific project “System Laptev Sea”.

References

Barnola, J. M., Raynaud, D., Neftel, A. and Oeschger, H.: Comparison of CO_2 measurements by two laboratories on air from bubbles in polar ice, Nature, 303(5916), 410–413, 1983.

Berg, T. E. and Black, R. F.: Preliminary measurements of growth of nonsorted polygons, Victoria Land, Antarctica, :InAntarctic Soils and Soil -Forming Processes, American Geophysical Union Antarctic Research Series, (1418), 61–108, 1966.

Black, R. F.: Permafrost - A review, Bulletin of the Geological Society of America, 65, 839–856, 1954.

Black, R. F.: Les coins de glace et le gel permanent dans le Nord de l'Alaska, Annales de Géographie, 72(391), 257–271, 1963.

Black, R. F.: Features indicative of permafrost, Annual Reviews Inc. Provided by the NASA Astrophysics Data System, 75–94, 1976.

Blunier, T., Chappellaz, J. A., Schwander, J., Barnola, J.-M., Desperts, T., Stauffer, B. and Raynaud, D.: Atmospheric methane record from a Greenland ice core over the last 1000 years, Geophysical Research Letters, 20(20), 2219–2222, 1993.

Bobrov, A. A., Muller, S., Chizhikova, N. A., Schirrmeister, L. and Andreev, A. A.: Testate amoebae in late quaternary sediments of the Cape Mamontov Klyk (Yakutia), Biol. Bull, 36(4), 363–372, 2009.

Brouchkov, A. and Fukuda, M.: Preliminary Measurements on Methane Content in Permafrost, Central Yakutia, and some Experimental Data, Permafrost and Periglacial Processes, 13, 187–197, 2002.

Cardyn, R., Clark, I. D., Lacelle, D., Lauriol, B., Zdanowicz, C. and Calmels, F.: Molar gas ratios of air entrapped in ice: A new tool to determine the origin of relict massive ground ice bodies in permafrost, Quaternary Research, 68(2), 239–248, 2007.

Clark, I. and Fritz, P.: Environmental isotopes in hydrogeology, CRC Press (Lewis Publishers)., 1997.

Corte, A. E.: Relationship between four ground patterns, structure of the active layer, and type and distribution of ice in the permafrost, U.S. Army Cold Regions Research and Engineering Laboratory., 1962.

Craig, H.: Isotopic variations in meteoric waters, Science, 133(3465), 1702–1703, 1961.

Dansgaard, W.: Stable isotopes in precipitation, Tellus, 16(4), 436–468, 1964.

Dereviagin, A. Y., Meyer, H., Chizhov, A. B., Hubberten, H.-W. and Simonov, E. F.: New data on the isotopic composition and evolution of modern ice wedges in the Laptev Sea region, Polarforschung, 70, 27–35, 2002.

Gell, W. A.: Underground Ice in Permafrost, Mackenzie Delta-Tuktoaktuk, N.W.T, 1976.

Gilichinsky, D. A., Nolte, E., Basilyan, A. E., Beer, J., Blinov, A. V., Lazarev, V. E., Kholodov, A. L., Meyer, H., Nikolskiy, P. A., Schirrmeister, L. and Tumskoy, V. E.: Dating of syngenetic ice wedges in permafrost with 36Cl, Quaternary Science Reviews, 26(11–12), 1547–1556, doi:10.1016/j.quascirev.2007.04.004, 2007.

IPCC: Climate change 2007: The physical Science Basis, Cambridge University Press., 2007.

Jacka, T. H.: Laboratory studies on relationships between ice crystal size and flow rate, Cold

Regions Science and Technology, 10(1), 31–42, 1984.

Johnsen, S. J., Dansgaard, W. and White, J. W. C.: The origin of Arctic precipitation under present and glacial conditions, Tellus, 41B, 452–468, 1989.

Jouzel, J., Masson-Delmotte, V., Stiévenard, M., Landais, A., Vimeux, F., J., S. J., Sveinbjornsdottir, A. and White, J. W. C.: Rapid deuterium-excess changes in Greenland ice cores : a link between the ocean and the atmosphere, C. R. Géoscience, 337, 957–969, 2005a.

Jouzel, J. and Merlivat, L.: Deuterium and oxygen 18 in precipitation: modeling of the isotopic effects during snow formation, Journal of Geophysical Research, 89, 11749–11757, 1984.

Jouzel, J., Merlivat, L. and Lorius, C.: Deuterium excess in an East Antarctic ice core suggests higher relative humidity at the oceanic surface during the last glacial maximum, Nature, 299, 688–691, 1982.

Jouzel, J., Stiévenard, M., Johnsen, S. J., Landais, A., Masson-Delmotte, V., Sveinbjornsdottir, A., Vimeux, F., von Grafenstein, U. and White, J. W. C.: The GRIP deuterium-excess record, Quaternary Science Reviews, 26(1-2), 1–17, 2005b.

Katayama, T., Tanaka, M., Moriizumi, J., Nakamura, T., Brouchkov, A., Douglas, T. A., Fukuda, M., Tomita, F. and Asano, K.: Phylogenetic analysis of bacteria preserved in a permafrost ice wedge for 25,000 years, Appl. Environ. Microbiol., 73(7), 2360–2363, 2007.

Killawee, J. A., Fairchild, I. J., Tison, J.-L., Janssens, L. and Lorrain, R.: Segregation of solutes and gases in experimental freezing of dilute solutions: Implications for natural glacial systems, Geochemica et Cosmochimica Acta, 62(23/24), 3637–3655, 1998.

Knight, P. G.: Glaciers, Stanley Thornes Ltd., 1999.

Kuznetsova, L. P.: Atmospheric moisture content and transfer over the territory of the former USSR, In Second International Workshop on Energy and Water Cycle in GAMESiberia, 1997, OhataT, HiyamaT (eds). Research Report of IHAS. Institute for Hydrospheric-Atmospheric Sciences, Nagoya University: Nagoya, Japan;, 145–151, 1998.

Lacelle, D., Radtke, K., Clark, I. D., Fisher, D., Lauriol, B., Utting, N. and Whyte, L. G.: Geomicrobiology and occluded O_2–CO_2–Ar gas analyses provide evidence of microbial respiration in ancient terrestrial ground ice, Earth and Planetary Science Letters, 306(1–2), 46–54, doi:10.1016/j.epsl.2011.03.023, 2011.

Lachenbruch, A. H.: Mechanics of thermal contraction cracks and ice wedge polygons in permafrost, Geological Society of America Special Papers, 70, 1–69, 1962.

Langway, C. C. J.: Ice fabrics and the universal stage, SIPRE Technical Report, 62, 1958.

Lauriol, B., Duchesne, C. and Clark, I. D.: Systématique du remplissage en Eau des Fentes de Gel: les Résultats d'une étude Oxygène-18 et Deutérium, Permafrost and Periglacial Processes, 6, 47–55, 1995.

Lawson, W.: Environmental Conditions, Ice Facies and Glacier Behaviour, in Glacier Science and Environmental Change, edited by P. G. Knight, pp. 319–328, Blackwell., 2007.

Mackay, J. R.: Ice-Wedge Cracks, Garry Island, Northwest Territories, Can. J. Earth Sci., 11(10), 1366–1383, doi:10.1139/e74-133, 1974.

Martinerie, P., Lipenkov, V. Y., Raynaud, D., Chappellaz, J., Barkov, N. I. and Lorius, C.: Air content paleo record in the Vostok ice core (Antarctica): A mixed record of climatic and glaciological parameters, J. Geophys. Res., 99(D5), 10565–10576, 1994.

Masson-Delmotte, V., Jouzel, J., Landais, A., Stievenard, M., Johnsen, S. J., White, J. W. C., Werner, M., Sveinbjornsdottir, A. and Fuhrer, K.: GRIP Deuterium Excess Reveals Rapid and Orbital-Scale Changes in Greenland Moisture Origin, Science, 309(5731), 118–121, 2005.

Merlivat, L. and Jouzel, J.: Global climatic interpretation of the deuterium-oxygen 18 relationship for precipitation., Journal of Geophysical Research, 84, 5029–5033, 1979.

Meyer, H., Dereviagin, A., Siegert, C., Schirrmeister, L. and Hubberten, H.-W.: Palaeoclimate Reconstruction on Big Lyakhovsky Island, North Siberia—Hydrogen and Oxygen Isotopes in Ice Wedges, Permafrost and Periglacial Processes, 13, 91–105, 2002a.

Meyer, H., Dereviagin, A. Y., Siegert, C. and Hubberten, H.-W.: Paleoclimate studies on Bykovsky Peninsula, North Siberia - hydrogen and oxygen isotopes in ground ice, Polarforschung, 70, 37–51, 2002b.

Meyer, H., Schirrmeister, L., Andreev, A., Wagner, D., Hubberten, H.-W., Yoshikawa, K., Bobrov, A., Wetterich, S., Opel, T., Kandiano, E. and Brown, J.: Lateglacial and Holocene isotopic and environmental history of northern coastal Alaska - Results from a buried ice-wedge system at Barrow, Quaternary Science Reviews, 29(27-28), 3720–3735, doi:doi: 10.1016/j.quascirev.2010.08.005, 2010a.

Meyer, H., Schirrmeister, L., Yoshikawa, K., Opel, T., Wetterich, S., Hubberten, H.-W. and Brown, J.: Permafrost evidence for severe winter cooling during the Younger Dryas in northern Alaska, Geophys. Res. Lett., 37(3), L03501, doi:10.1029/2009GL041013, 2010b.

Meyer, H., Schönicke, L., Wand, U., Hubberten, H.-W. and Friedrichsen, H.: Isotope studies of hydrogen and oxygen in ground ice—Experiences with the equilibration technique, Isotopes in environmental and health studies, 36, 133–149, 2000.

Michel, F. A.: Isotope investigations of permafrost waters in northern Canada, University of Waterloo, Ontario, Canada, Dept. of Earth Sciences., 1982.

Moser, H. and Stichler, W.: Environmental isotopes in ice and snow, in Handbook of Environmental Isotope Geochemistry, the terrestrial environment, 1A, edited by P. Fritz and J. Fontes, pp. 141–178, Elsevier, Amsterdam., 1980.

Müller, S., Bobrov, A. A., Schirrmeister, L., Andreev, A. A. and Tarasov, P. E.: Testate amoebae record from the Laptev Sea coast and its implication for the reconstruction of Late Pleistocene and Holocene environments in the Arctic Siberia, Palaeogeography, Palaeoclimatology, Palaeoecology, 271(3-4), 301–315, 2009.

Opel, T., Dereviagin, A. Y., Meyer, H., Schirrmeister, L. and Wetterich, S.: Palaeoclimatic information from stable water isotopes of Holocene ice wedges on the Dmitrii Laptev Strait, northeast Siberia, Russia, Permafrost Periglac. Process., 22(1), 84–100, doi:10.1002/ppp.667, 2011.

Paterson, W. S. B.: The physics of glaciers, third edition, Butterworth-Heinemann, Oxford., 1994.

Pickering, F. B.: The basis of Quantificative Metallography., Metals and Metallurgy Trust., 1976.

Popp, S., Diekmann, B., Meyer, H., Siegert, C., Syromyatnikov, I. and Hubberten, H.-W.: Palaeoclimate Signals as Inferred from Stable-isotope Composition of Ground Ice in the Verkhoyansk Foreland, Central Yakutia, Permafrost and Periglacial Processes, 17, 119–132, 2006.

Raffi, R., Stenni, B., Flora, O., Polesello, S. and Camusso, M.: Growth processes of an inland

Antarctic ice wedge, Mesa Range, northern Victoria Land, Annals of Glaciology, 39(1), 379–385, doi:10.3189/172756404781814195, 2004.

Raynaud, D., Chapellaz, J., Barnola, J. M., Korotkevich, Y. and Lorius, C.: Climatic and CH4 cycle implications of glacial-interglacial CH_4 change in the Vostok ice core, Nature, 333(6174), 655–657, 1988.

Raynaud, D., Delmas, D., Ascencio, J. M. and Legrand, M.: Gas extraction from polar ice cores: a critical issue for studying the evolution of atmospheric CO_2 and ice-sheet surface elevation, Annals of Glaciology, 3, 265–268, 1982.

Rinke, A., Dethloff, K., Spekat, A., Enke, W. and Hesselbjerg Christensen, J.: High resolution climate simulations over the Arctic, Polar Research; Vol 18, No 2 (1999): Special issue: Proceedings of the International Symposium on Polar Aspects of Global Change [online] Available from: http://www.polarresearch.net/index.php/polar/article/view/6567, 1999.

Romanosky, N. N.: The scheme of correlation of polygonal wedge structures, Biuletyn Peryglacjalny, (26), 287–294, 1976.

Samyn, D., Fitzsimons, S. and Lorrain, R.: Strain-induced phase changes within cold basal ice from Taylor Glacier, Antarctica, indicated by textural and gas analyses, Journal of Glaciology, 51(175), 611–619, 2005.

Schirrmeister, L., Grosse, G., Kunitsky, V., Magens, D., Meyer, H., Dereviagin, A., Kuznetsova, T., Andreev, A., Babiy, O., Kienast, F., Grigoriev, M., et al.: Periglacial landscape evolution and environmental changes of Arctic lowland areas for the last 60,000 years (Western Laptev Sea coast, Cape Mamontov Klyk), Polar Research, 27(2), 249–272, 2008.

Schirrmeister, L., Siegert, C., Kuznetsova, T., Kuzmina, S., Andreev, A., Kienast, F., Meyer, H. and Bobrov, A.: Paleoenvironmental and paleoclimatic records from permafrost deposits in the Arctic region of Northern Siberia, Quaternary International, 89, 97–118, 2002.

Schwamborn, G., Meyer, H., Fedorov, G., Schirrmeister, L. and Hubberten, H.-W.: Ground ice and slope sediments archiving late Quaternary paleoenvironment and paleoclimate signals at the margins of El'gygytgyn Impact Crater, NE Siberia, Quaternary Research, 66(2), 259–272, doi:10.1016/j.yqres.2006.06.007, 2006.

Souchez, R., Janssens, L., Lemmens, M. and Stauffer, B.: Very low oxygen concentration in basal ice from Summit, Central Greenland, Geophysical Research Letters, 22(15), 2001–2004, 1995a.

Souchez, R., Jouzel, J., Landais, A., Chapellaz, J., Lorrain, R. and Tison, J.-L.: Gas isotopes in ice reveal a vegetated central Greenland during ice sheet invasion, Geophysical Research Letters, 33, L24503, doi:10.1029/2006GL028424, 2006.

Souchez, R., Lemmens, M. and Chapellaz, J.: Flow-induced mixing in the GRIP basal ice deduced from the CO2 and CH4 records, Geophysical Research Letters, 22(1), 41–44, 1995b.

Souchez, R. and Lorrain, R.: Ice Composition and Glacier Dynamics, Springer-Verlag., 1991.

Stenni, B., Jouzel, J., Masson-Delmotte, V., Röthlisberger, R., Castellano, E., Cattani, O., Falourd, S., Johnsen, S. J., Longinelli, A., Sachs, J. P., Selmo, E., et al.: A late-glacial high-resolution site and source temperature record derived from the EPICA Dome C isotope records (East Antarctica), Earth and Planetary Science Letters, 217(1-2), 183–195, 2004.

Stenni, B., Masson-Delmotte, V., Johnsen, S., Jouzel, J., Longinelli, A., Monnin, E., Röthlisberger, R. and Selmo, E.: An Oceanic Cold Reversal During the Last Deglaciation,

Science, 293(5537), 2074–2077, 2001.

Steven, B., Pollard, W. H., Greer, C. W. and Whyte, L. G.: Microbial diversity and activity through a permafrost/ground ice core profile from the Canadian high Arctic, Environmental Microbiology, 10(12), 3388–3403, doi:10.1111/j.1462-2920.2008.01746.x, 2008.

St-Jean, M., Lauriol, B., Clark, I. D., Lacelle, D. and Zdanowicz, C.: Investigation of ice-wedge infilling processes using stable oxygen and hydrogen isotopes, crystallography and occluded gases (O_2, N_2, Ar), Permafrost Periglac. Process., 22(1), 49–64, doi:10.1002/ppp.680, 2011.

Tison, J.-L.: Diamond -wire saw cutting technique for investigating textures and fabrics of debris-laden ice and brittle ice, J. Glaciol., 40(135), 410 – 414, 1994.

Tison, J.-L., Souchez, R., Wolff, E. W., Moore, J. C., Legrand, M. R. and de Angelis, M.: Is a periglacial biota responsible for enhanced dielectric response in basal ice from the Greenland Ice Core Project ice core?, Journal of Geophysical Rese arch, 1998, 103(D15), 18885–18894, 1998.

Vaikmäe, R.: Oxygen isotopes in permafrost and ground ice - a new tool for paleoclimatic investigations, Leipzig., 1989.

Vasil'chuk, Y. K. and Vasil'chuk, A. C.: Oxygen-isotope and C^{14} data associated with Late Pleistocene syngenetic ice-wedges in mountains of Magadan region, Siberia, Permafrost and Periglacial Processes, 9(2), 177–183, 1998.

Vimeux, F., Cuffey, K. and Jouzel, J.: New insights into Southern Hemisphere temperature changes from Vostok ice cores using deuterium excess correction over the Last 420,000 Years, Earth and Planetary Science Letters, 203(3-4), 829–843, 2002.

Vimeux, F., Masson-Delmotte, V., Jouzel, J., Stiévenard, M. and Petit, J. R.: Glacial-interglacial changes in ocean surface conditions in the southern Hemisphere, Nature, 398, 410–413, 1999.

Wagner, D. and Liebner, S.: Global warming and carbon dynamics in permafrost soils: Methane production and oxidation, in Permafrost Soils, edited by R. Margesin, pp. 219–236, Springer Berlin Heidelberg., 2009.

Wetterich, S., Kuzmina, S., Andreev, A. A., Kienast, F., Meyer, H., Schirrmeister, L., Kuznetsova, T. and Sierralta, M.: Palaeoenvironmental dynamics inferred from late Quaternary permafrost deposits on Kurungnakh Island, Lena Delta, Northeast Siberia, Russia, Quaternary Science Reviews, 27(15-16), 1523–1540, 2008.

Wetterich, S., Rudaya, N., Tumskoy, V., Andreev, A. A., Opel, T., Schirrmeister, L. and Meyer, H.: Last Glacial Maximum records in permafrost of the East Siberian Arctic, Quaternary Science Reviews, 30(21–22), 3139–3151, doi:10.1016/j.quascirev.2011.07.020, 2011.

Yershov, E. D.: Geokryologija SSSR (Geocryology of the USSR), Nedra, Moscow., 1989.

Yurtsever, Y. and Gat, J. R.: Atmospheric waters, in Stable Isotope Hydrology: Deuterium and Oxygen in Water Cycle, edited by T. Rep., pp. 103–145, IAEA, Vienna., 1981.

Zeebe, R. E. and Wolf-Gladrow, D.: CO_2 in Seawater: Equilibrium, Kinetics, Isotopes, 65, Elsevier., 2001.

Table 1. Summary of results and comparison between IW-26, ISW-28 and IW-28. ~~and comparison with the atmosphere and the meteoric ice~~. Values separated with / are the minimum and the maximum, ~~the number between~~ (number) corresponds to ~~the~~ mean values.

	IW-26	ISW-28	IW-28
Crystal area range (mm²)	10.18 – 27.34	4.15 – 9.62	0.95 – 4.15
Crystal shape	equigranular	granular/rectangular elongated vertically sediments at grain boundary	equigranular
c-axes	1 max in horizontal girdle	horizontal girdle	1 max in horizontal girdle
Bubble size	~1mm	~1mm	~1mm
Bubble shape	spherical	spehrical	spherical
Total gas content (ml/kg) (Meteoric ice =75-140*)	10/36 (homogeneous) (27)	11/42 (heterogeneous) (25)	27/50 (homogeneous) (45)
N_2 (%)	77/86 (82)	78/89 (85)	82/89 (86)
O_2 (%)	5/13 (10)	10/21 (15)	10/13 (12)
Ar (%)	(1.16)	(1.03)	(0.93)
CO_2 (ppmV)	35 000/110 000 (62 000)	860/7000 (3000)	10 000/48 000 (25 000)
CH_4 (ppmV)	0.5/1.6 (1)	41/72 (55)	7/10 (8)
$\delta^{18}O$ (‰)	-30.6/-22.6 (-24.9)	-30.9/-28.9 (-29.9)	-31.9/-29.4 (-31)
δD (‰)	- 230/- 170 (-188)	-246/-230 (-237)	-247/-229 (-240)
$\delta^{18}O/\delta D$ slope (‰)	6.63 (r^2=0.94)	8.03 (r^2=0.98)	7.44 (r^2=0.98)

*Martinerie et al. (1992)

Table 2: Comparison of relative values of δ, *d* and precipitation amount for the two sections of ice wedge ISW-28/IW-28 with expected values for the two atmospheric moisture sources hypotheses discussed in the text.

(1)	(2)	(3)	(4)	(5)	(6)	(7)
variables	Hyp. 1: Atlantic source		Hyp. 2: Atlantic vs. North Pacific		ISW-28	IW-28
	low sea ice Interstadial	high sea ice Stadial	Interstadial	Stadial		
δ-values (T° site)	high	low	high	low	low	lower
d-values (T° source)	**low**	high	high	**low**	**low**	high
Precipitation (distance controlled)	high	low	high	low	low	high

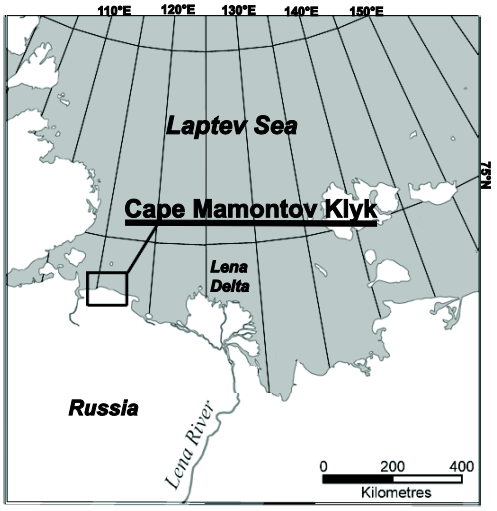

Figure 1: Location of the Cape Mamontov Klyk sampling site in Arctic Siberia. The studied ice wedges were exposed on a coastal cliff on the Laptev Sea coast.

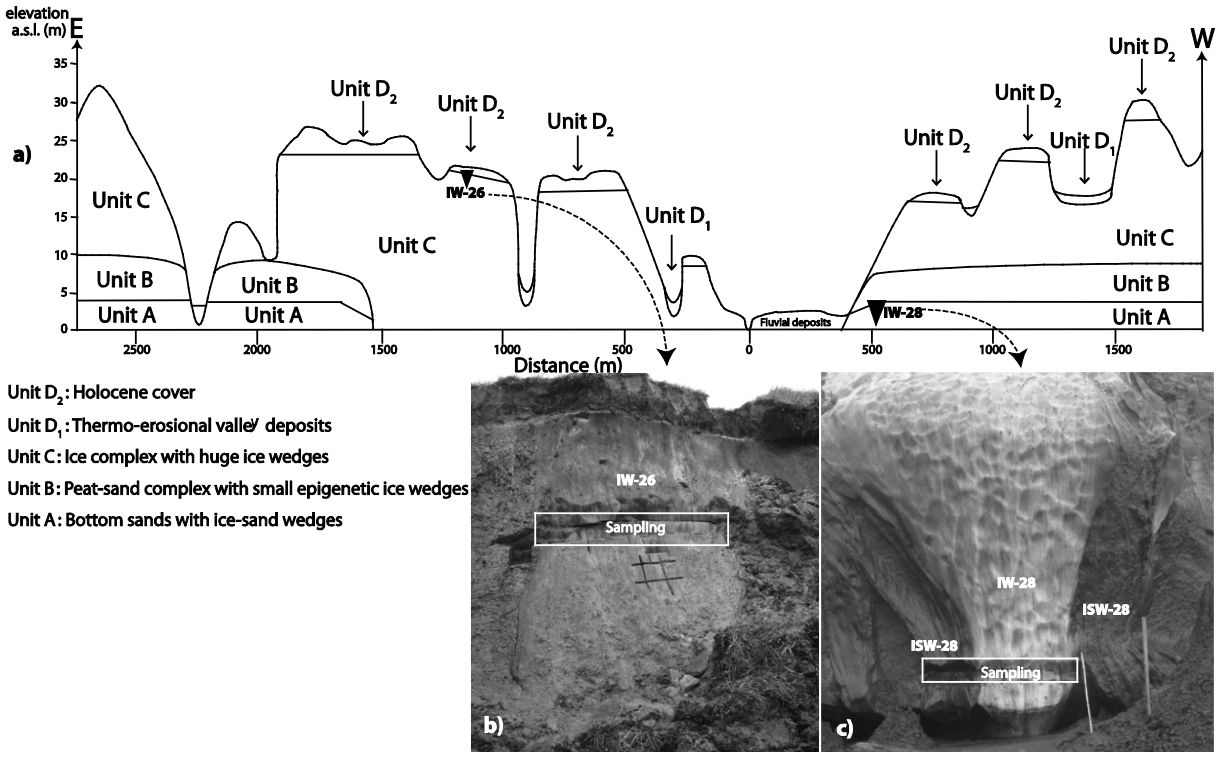

Figure 2: a) General stratigraphic scheme of the main section of Mamontov Klyk (adapted from Schirrmeister et al., 2008)~~(adapted from Schirrmeister et al., 2008)~~ with positions and ~~the~~ general settings b) and c) of ice wedges 26 (IW-26) and 28 (IW-28) respectively. The sampling areas are outlined with white boxes, on approximately 160 cm and 190 cm for respectively IW-26 and IW-28. Rectangular parallelepipeds have been removed from the cliff with chain-saw of which the upper part (1.5 cm thickness) has been used in this work. Note that IW-28 was sampled in both the ice-sand wedge (ISW-28, left of box) and in the ice wedge itself (IW-28, right of box).

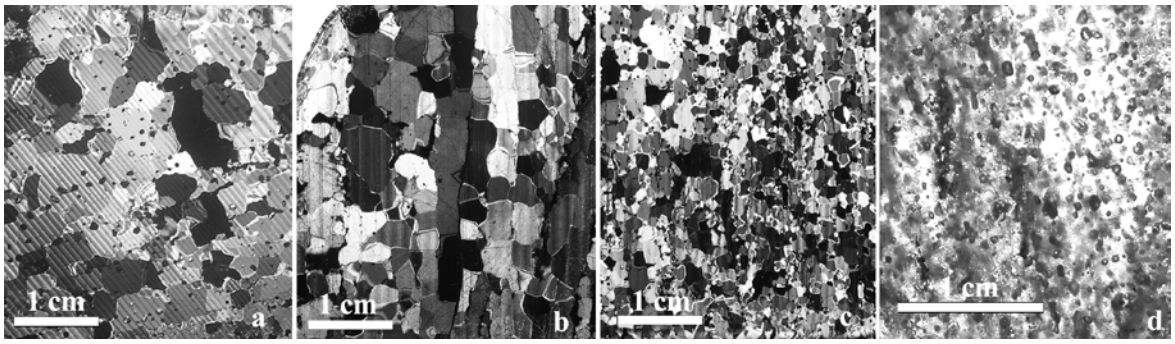

Figure ~~4~~3: Thin section photographs of the textural properties of the ice wedges. a) IW-26, b) ISW-28 (ice-sand wedge), the left part of ice wedge 28 with debris sub vertical layers (note the crystal elongation along the foliation), c) IW-28, clean ice in the central part of ice wedge 28 and d) thick section photograph of ice from IW-28 in transmitted light allowing bubble content observation.

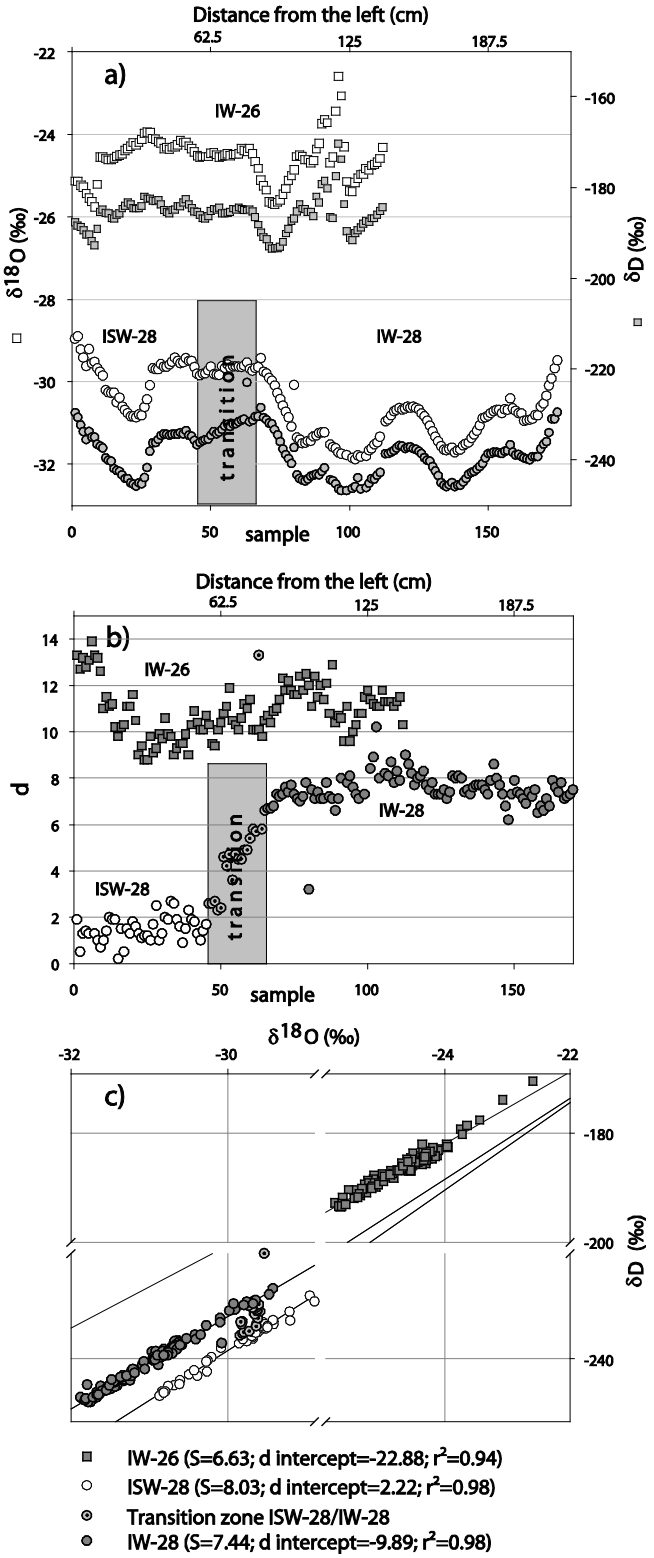

Figure ~~3~~4: Isotopic data for the two ice wedges: a) $\delta^{18}O$ and δD profiles, b) *d* and c) $\delta^{18}O$-δD relationship. Numbers on the bottom x-axis~~coordinate~~ of a) and b) refer to ice sample ordering, increasing from left to right, in the outcrop. The equivalent horizontal distance from extreme left is shown on the upper x-axis.

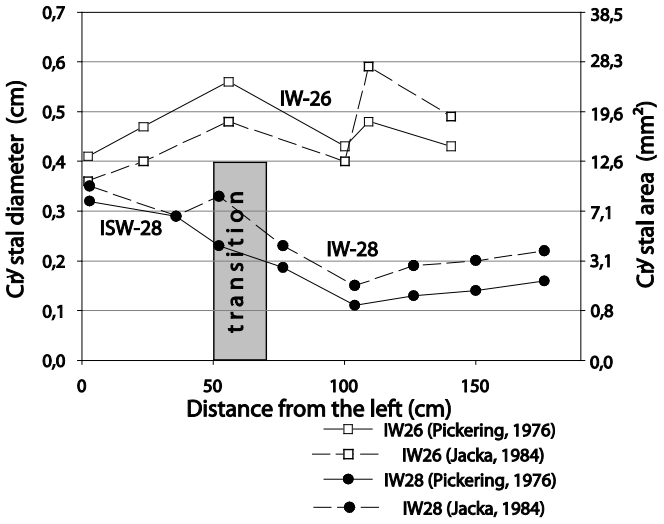

1

2 Figure 5: Crystals size measurements using the two techniques described in the “sampling and
3 analytical methods” section.

4

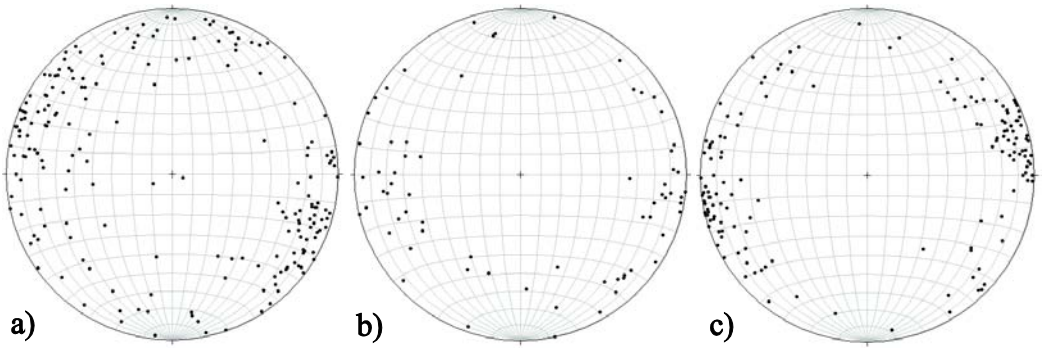

Figure 6: Schmidt equal-area diagrams for the c-axes of horizontal thin sections. a) a total of six thin sections from IW-26 (n = 199) showing horizontal girdle with 1 maximum, b) a total of two thin sections from ISW-28 (n = 70) showing horizontal girdle, c) a total of five thin sections from IW-28 (n = 150) showing horizontal girdle with 1 maximum.

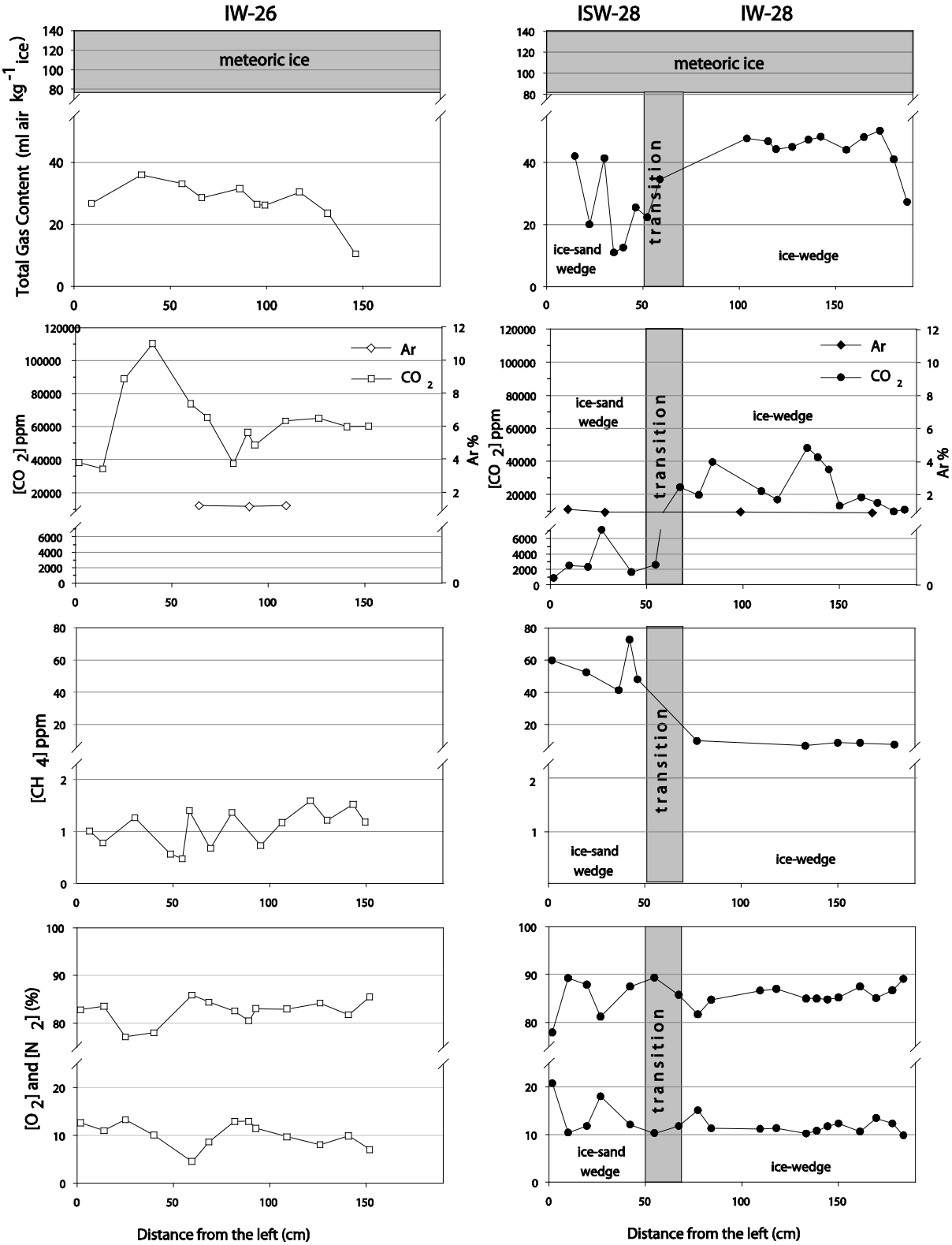

Figure 7: Gas properties of ice wedges IW-26 (left) and ISW-28/IW-28 (right).

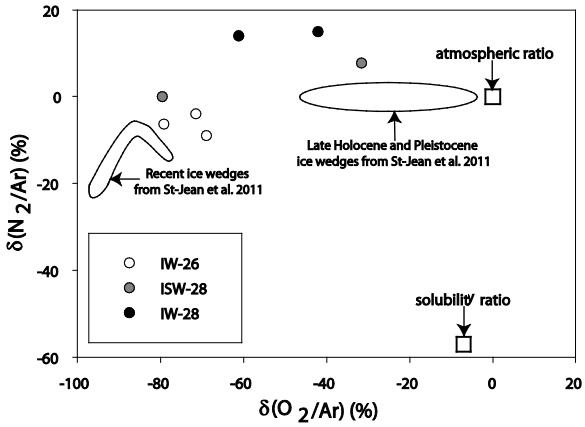

Figure 8: $\delta(N_2/Ar)$ and $\delta(O_2/Ar)$ of ice wedges IW-26, ISW-28 and IW-28 using the following equation: $\delta(N_2/Ar) = \left(\frac{R(N_2/Ar)_{sa}}{R(N_2/Ar)_{st}} - 1\right) * 100$ where *sa* refers to the sample and *st* to the standard value (standards used are 22.43 and 83.60 for O_2/Ar and N_2/Ar, respectively). An equivalent formula is used for determining $\delta(O_2/Ar)$.

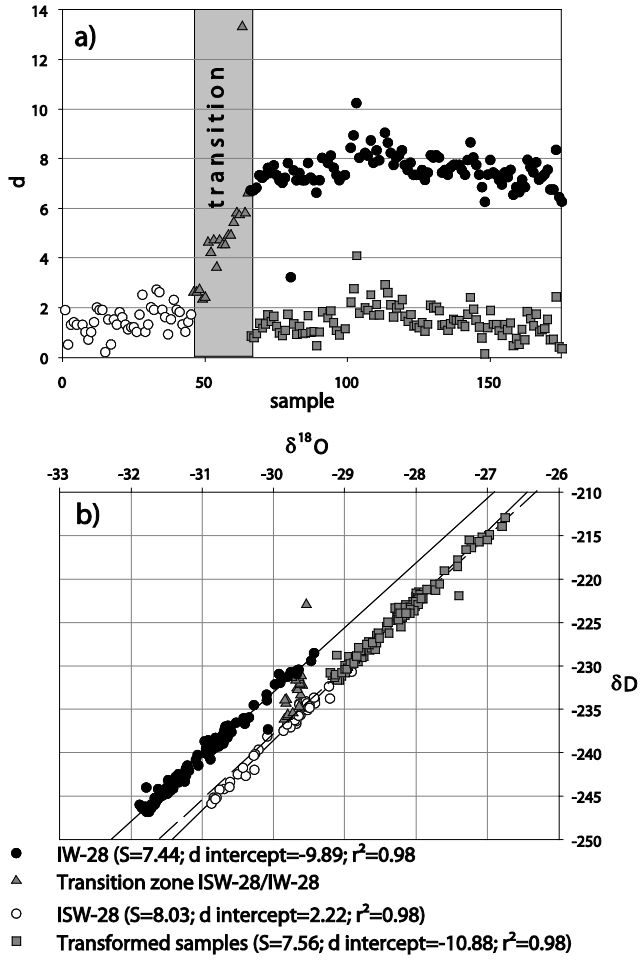

Figure ~~8~~9: *d* (a) and co-isotopic plots (b) of observed data for ISW-28 (open circles) and IW-28 (black dots) compared to a simulation (grey squares) on the effect of hypothetical equilibrium refreezing of 10% of melted fraction in IW-28 sample, using Eq. (1). The refrozen theoretical IW-28 samples reproduce the *d* of the ISW-28 samples and lie on the same co-isotopic line. They are however clearly offset towards less negative δ values.~~(see text for details).~~